(23) B. R. McGarvey, *J. Phys. Chem.*, 71, 51 (1967).
(24) D. P. Bakalik and R. G. Hayes, *Inorg. Chem.*, 11, 1734 (1972). The χ value of −2.08 was calculated from the isotropic coupling constant from the solution EPR spectrum of $V(\eta^5\text{-}C_5H_5)_2Cl_2$ rather than from single-crystal EPR data.
(25) J. L. Petersen, D. L. Lichtenberger, R. F. Fenske, and L. F. Dahl, *J. Am. Chem. Soc.*, 97, 6433 (1975).
(26) B. R. McGarvey in "Electron Spin Resonance of Metal Complexes", Teh Fu Yen, Ed., (Plenum Press, New York, N.Y., 1969); from the Symposium of ESR on Metal Chelates at the Pittsburgh Conference on Analytical Chemistry and Applied Spectroscopy, Cleveland, Ohio, March 1968.
(27) J. S. Griffith, "The Theory of Transition Metal Ions", Cambridge, England, 1964 p 427.
(28) $|\Psi_0\rangle = -0.500d_{z^2} - 0.866d_{x^2-y^2}$ with respect to a left-handed coordinate system where the z axis is normal to the ML_2 plane.
(29) Previously reported values[11] of K, P, $\langle r^{-3}\rangle$, and χ are too large by ca. 7% due to the earlier use of an approximate conversion factor.
(30) Reference 14, p 706.
(31) Reference 14, p 399.
(32) T. M. Dunn, *Trans. Faraday Soc.*, 57, 1441 (1961).

Synthesis and Structural Characterization by X-Ray Diffraction and Electron Paramagnetic Resonance Single-Crystal Techniques of $V(\eta^5\text{-}C_5H_4CH_3)_2Cl_2$ and $Ti(\eta^5\text{-}C_5H_4CH_3)_2Cl_2$. A Study of the Spatial Distribution of the Unpaired Electron in a $V(\eta^5\text{-}C_5H_5)_2L_2$-Type Complex[1]

Jeffrey L. Petersen and Lawrence F. Dahl*

Contribution from the Department of Chemistry, University of Wisconsin, Madison, Wisconsin 53706. *Received February 24, 1975*

Abstract: The preparation of $Ti(\eta^5\text{-}C_5H_4CH_3)_2Cl_2$ and $V(\eta^5\text{-}C_5H_4CH_3)_2Cl_2$ and subsequent characterization by single-crystal X-ray diffraction and EPR methods were performed in order to delineate more clearly the bonding description of the unpaired electron in a V(IV) $V(\eta^5\text{-}C_5H_5)_2L_2$ complex upon change of the L ligands. The results of this work not only have substantiated our earlier EPR study of $V(\eta^5\text{-}C_5H_5)_2S_5$ but also have contributed to a more general understanding of the nature of bonding in $M(\eta^5\text{-}C_5H_5)_2L_2$ complexes. An EPR measurement of $V(\eta^5\text{-}C_5H_4CH_3)_2Cl_2$ (of crystallographic C_2-2 symmetry per se) diluted in the crystal lattice of $Ti(\eta^5\text{-}C_5H_4CH_3)_2Cl_2$ (of crystallographic C_s-m site symmetry) has shown that the anisotropy in the ^{51}V hyperfine coupling interaction arises primarily from the significantly different vanadium orbital character of $3d_{z^2}$ and $3d_{x^2-y^2}$ AO's comprising the a_1-type MO containing the unpaired electron. The similarity between the EPR results for $V(\eta^5\text{-}C_5H_5)_2S_5$ and $V(\eta^5\text{-}C_5H_4CH_3)_2Cl_2$ supports the premise that the metal orbital characters of the unpaired electron are not strongly dependent on the nature of the L ligands. The g and hyperfine tensors in $V(\eta^5\text{-}C_5H_4CH_3)_2Cl_2$ (for which $g_x = 1.9802$, $g_y = 1.9695$, $g_z = 2.0013$; $T_x = (-)80.6$ G, $T_y = (-)125.5$ G, $T_z = (-)20.6$ G) are coincident, and the orientation of their principal axial directions is identical with the orientation of the principal axial directions of the hyperfine tensor in $V(\eta^5\text{-}C_5H_5)_2S_5$. The prominent crystallographic differences between $Ti(\eta^5\text{-}C_5H_4CH_3)_2Cl_2$ and $V(\eta^5\text{-}C_5H_4CH_3)_2Cl_2$ are: (1) a Cl-V-Cl bond angle of 87.1 (1)° being 6° smaller than the Cl-Ti-Cl bond angle of 93.2 (1)° and (2) the one independent V-Cl bond length of 2.398 (2) Å being 0.04 Å *longer* than the average Ti-Cl bond length of 2.360 (2) Å, in contradistinction to the average V-C distance being 0.05 Å *shorter* than the average Ti-C distance. These reversed bond-length trends, which are likewise observed between the titanium and vanadium molecules with phenyl mercaptide and pentasulfide ligands, are in harmony with the unpaired electron in each V(IV) complex occupying a MO which is antibonding with respect to the V-L bonds. $Ti(\eta^5\text{-}C_5H_4CH_3)_2Cl_2$ crystallizes with four molecules in an orthorhombic unit cell of symmetry *Pnma* with $a = 11.928$ (5), $b = 15.147$ (6), and $c = 6.848$ (4) Å, while $V(\eta^5\text{-}C_5H_4CH_3)_2Cl_2$ crystallizes with four molecules in a monoclinic unit cell of symmetry $C2/c$ with $a = 13.614$ (2) Å, $b = 6.720$ (1) Å, $c = 13.763$ (2) Å, and $\beta = 105.99$ (1)°. Final full-matrix least-squares refinement which utilized anisotropic thermal parameters for all nonhydrogen atoms gave $R_1 = 4.6\%$ and $R_2 = 6.2\%$ for $Ti(\eta^5\text{-}C_5H_4CH_3)_2Cl_2$ and $R_1 = 4.1\%$ and $R_2 = 4.8\%$ for $V(\eta^5\text{-}C_5H_4CH_3)_2Cl_2$.

Structural determinations by X-ray diffraction[2] of the paramagnetic $V(\eta^5\text{-}C_5H_5)_2L_2$-type complexes and the analogous titanium complexes provided an operational test of the Ballhausen-Dahl bonding description[3] applied to $M(\eta^5\text{-}C_5H_5)_2L_2$ complexes. The salient structural feature resulting from these crystallographic studies was that the similar L-M-L bond angles in the d^1 V(IV) complexes were found to be ca. 6° *less* than those in the corresponding d^0 Ti(IV) complexes. This structural incompatibility of the L-M-L bond angles with the B-D model was taken as prime evidence by us[2,4] for its general invalidity for $M(\eta^5\text{-}C_5H_5)_2L_2$-type complexes. The paramagnetism of $V(\eta^5\text{-}C_5H_5)_2S_5$ along with the existence of the diamagnetic $Ti(\eta^5\text{-}C_5H_5)_2S_5$ complex provided an opportunity to employ dilute single-crystal electron paramagnetic resonance to determine quantitatively the metal orbital character as well as the directional properties of the molecular orbital containing the unpaired electron in a $V(\eta^5\text{-}C_5H_5)_2L_2$-type complex. This work[5] disclosed that the unpaired electron in $V(\eta^5\text{-}C_5H_5)_2S_5$ resides primarily on the vanadium atom in an a_1-type molecular orbital which consists mainly of $3d_{z^2}$ with a small but significant amount of $3d_{x^2-y^2}$ and negligible 4s character (i.e., with respect to a right-handed Cartesian coordinate system for which z is directed normal to the xy plane which bisects the VS_2 bond angle, and x lies along the line of the VS_2 bisector). This EPR study provided the first quantitative evidence for the demise of the Ballhausen-Dahl model as a valid bonding description for $M(\eta^5\text{-}C_5H_5)_2L_2$ complexes.

Since the isotropic hyperfine coupling constants for a large number of $V(\eta^5\text{-}C_5H_5)_2L_2$ (L = Cl, SH, OCN, CN, SeCN, N_3, SCN) complexes fall within the range of 60–75

Table I. Solid-State Infrared Spectra of $M(\eta^5\text{-}C_5H_5)_2Cl_2$ and $M(\eta^5\text{-}C_5H_4CH_3)_2Cl_2$ (M = Ti, V)[a,b]

$Ti(\eta^5\text{-}C_5H_5)_2Cl_2$	$V(\eta^5\text{-}C_5H_5)_2Cl_2$	$Ti(\eta^5\text{-}C_5H_4CH_3)_2Cl_2$	$V(\eta^5\text{-}C_5H_4CH_3)_2Cl_2$	Assignment
(m) 3123	(m) 3098	(m) 3109	(m) 3100	C–H str (ν(CH))
		(m) 2924	(m) 2920	C–H str ($\nu(CH_3)$)
		(b) 1632	(b) 1630	C–C str
		(s) 1503	(s) 1493	asym ($\delta_{as}(CH_3)$)
(m) 1439	(m) 1439	(m) 1452	(m) 1450	C–C str (ω(CC))
		1444	1438	
		1420		
(w) 1362	(w) 1366	(s) 1371	(m) 1362	C–C str (ω(CC))
		(w) 1255	(b) 1250	CH_3 wag
		(w) 1245		
(w) 1129	(w) 1122			
		(w) 1080		
(w) 1027	(w) 1022	(s) 1053	(m) 1050	C–H def (δ(CH))
(m) 1011	(w) 1007	(m) 1040	(m) 1040	C–H def (δ(CH))
		(m) 1030		
(w-b) 923	(m-b) 989	(w) 936	(w) 920	
		(w) 900		
(m) 871	(m) 878	(sh) 870	(sh) 860	C–H def (γ(CH))
		(s) 858	(s) 850	
(s) 818	(s) 823	(m) 822	(s) 829	C–H def (γ(CH))

[a] Key: s, strong; m, moderate; w, weak; sh, shoulder; v, very; b, broad. [b] All values are in units of cm^{-1}.

G,[2b,6] they apparently indicate a similar behavior of the unpaired electron in these complexes despite a considerable variation in the nature of the terminal ligands L. To determine whether or not a significant change occurs in the metal orbital character of the unpaired electron upon substitution of the more electronegative chlorine ligands for the pentasulfide bidentate ligand, the preparation and characterization by single-crystal X-ray and EPR methods of $V(\eta^5\text{-}C_5H_4CH_3)_2Cl_2$ and $Ti(\eta^5\text{-}C_5H_4CH_3)_2Cl_2$ were undertaken.[7,8] Besides providing an opportunity to test the conclusions of the dilute single-crystal EPR study of $V(\eta^5\text{-}C_5H_5)_2S_5$, the resulting work presented here has contributed to a more general understanding of the nature of bonding in these $M(\eta^5\text{-}C_5H_5)_2L_2$-type molecules.

Experimental Section

Preparation. Bis(methylcyclopentadienyl)titanium dichloride and bis(methylcyclopentadienyl)vanadium dichloride were prepared by the reaction of stoichiometric quantities of sodium methylcyclopentadienide with the appropriate metal tetrachloride.[9] Sodium methylcyclopentadienide was prepared by a slow reaction of freshly cracked methylcyclopentadiene (Aldrich Chemical Co.) with a fine dispersion of Na metal in glyme under a nitrogen atomsphere. The resulting violet solution was added dropwise under nitrogen to a dry benzene solution of a metal tetrachloride (Alfa Inorganics, Inc.). Once the reaction mixture had cooled, the excess solvent was removed by rotary evaporation. The residue was placed in a large cellulose thimble of a Sohxlet extractor and the reaction product extracted with chloroform. Cooling of the chloroform solution led to the formation of small crystals of the $M(\eta^5\text{-}C_5H_4CH_3)_2Cl_2$ derivative which were collected by filtration and washed with pentane and small amounts of ethanol and acetone.

Physical Properties. A Digilab FTS-20 infrared spectrometer was used to obtain ir spectra from KBr disks containing the methylcyclopentadienyl compounds. Spectra, averaged for 40 scans, were obtained with a resolution setting of 4 cm^{-1} over the selected scan range of 3800–600 cm^{-1}. The ir spectra for $M(\eta^5\text{-}C_5H_4CH_3)_2Cl_2$ are compared to those[2a] for $M(\eta^5\text{-}C_5H_5)_2Cl_2$ in Table I, where M = Ti, V. The spectra are quite similar except that the methyl substituent of each cyclopentadienyl ring introduces extra vibrational structure due to the C–H stretch, C–C stretch, C–C asymmetric bend, and CH_3 wag which are located at ca. 2920, 1630, 1500, and 1250 cm^{-1}, respectively.

The ^1H NMR solution spectrum of $Ti(\eta^5\text{-}C_5H_4CH_3)_2Cl_2$ dissolved in acetone-d_6 was recorded on a Varian XL-100 spectrometer at room temperature with the radiofrequency set at 100.1 MHz. The spectrum contains three groups of peaks in the ratio 3:2:2 due to the three types of protons on the methylcyclopentadienyl rings. The methyl protons show up as one single line at δ 2.32. For the remaining four ring protons, H(2) and H(5) are designated as the α-protons and H(3) and H(4) as the β-protons. The ^1H lines for the α- and β-protons are shifted to δ 7.40 and 7.66, respectively. Each of these lines is characterized by an apparent triplet with relative intensities of 1:2:1. These triplets arise from the proton coupling of $J_{\alpha\beta}$ = 1.3 Hz between the α- and β-protons.

Table II. Magnetic Susceptibility Data for $V(\eta^5\text{-}C_5H_4CH_3)_2Cl_2$

T (°K)	$10^6\chi_g$ (cgsu/g)[a]	$10^4\chi_m^{corr}$ (cgsu/mol)	$\mu_{eff} = 2.828(\chi_m^{corr}T)^{1/2}$
84.8	11.9[b]	35.3[b]	1.55[b]
94.5	11.80	35.04	1.63
104.2	10.95	32.66	1.65
113.9	10.07	30.20	1.66
129.8	8.82	26.70	1.66
145.2	7.90	24.12	1.67
160.4	7.08	21.82	1.67
176.0	6.42	19.97	1.68
192.0	5.85	18.4	1.68
208.2	5.36	17.0	1.68
224.1	4.96	15.9	1.69
240.3	4.59	14.8	1.69
256.6	4.29	14.0	1.70
273.2	3.99	13.2	1.70
295.3	3.67	12.2	1.70

[a] χ_g is the gram susceptibility calculated from the relationship $\chi_g = g\Delta w/wH(dH/dz) = b\Delta w/w$, where w is the sample weight, Δw the weight change, and b is a constant which depends upon the field characteristics; $\chi_m^{corr} = Ng^2\mu_{eff}^2\beta^2/3k(T-\theta) = C/(T-\theta)$; $\mu_{eff} = 2.828[\chi_m^{corr}(T-\theta)]^{1/2} = 1.73$ BM; $\mu_{eff}^{295} = 2.828(\chi_m^{corr}T)^{1/2} = 1.70$ BM. [b] Field dependence noted at this temperature. The value which is given here was found by extrapolation to $1/H = 0$ for a plot of χ_g vs. $1/H$ (method discussed by K. Honda, *Ann. Phys.*, 32, 1027 (1910), and M. Owen, *ibid.*, 37, 657 (1912).

The magnetic susceptibility data presented in Table II for $V(\eta^5\text{-}C_5H_4CH_3)_2Cl_2$ were obtained in a temperature range of 85–295 K via a Faraday apparatus.[10] A sample weighing 14.12 mg was sealed in a 28.14-mg Pyrex bulb.[11] The gram susceptibility at each temperature was selected as the average of the values for five different magnetic field strengths between 6 and 8 Oe. Corrections for the glass were made by a repetition of the susceptibility measurements of the container at all 15 temperatures and five field strengths after the sample had been removed. A diamagnetic correction[12] for the ligands and the core electrons of -199×10^{-6} cgsu/mol was applied to the molar susceptibility. In this temperature range, $V(\eta^5\text{-}C_5H_4CH_3)_2Cl_2$ follows the Curie-Weiss law, $\chi_m^{corr} = C/(T-\theta)$, where $C = Ng^2\mu_{eff}^2\beta^2/3k$. The values for the effective magnetic moment, μ_{eff}, and θ as determined from least-squares analysis of the plot of $1/\chi_m^{corr}$ vs. T (°K) are 1.73 BM and −10°, respectively.

The solution EPR spectrum of $V(\eta^5\text{-}C_5H_4CH_3)_2Cl_2$ dissolved in chloroform is shown in Figure 1. The eight-line spectrum, which

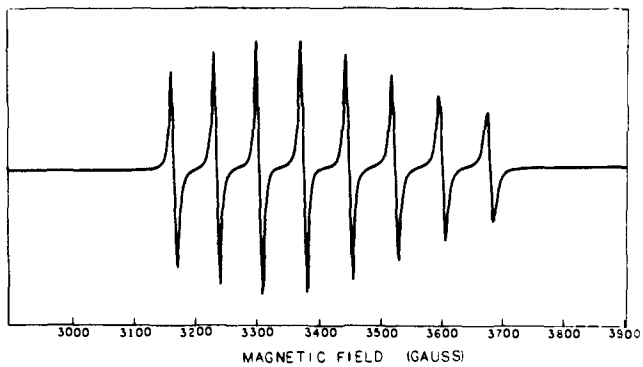

Figure 1. Solution EPR spectrum of $V(\eta^5\text{-}C_5H_4CH_3)_2Cl_2$ in chloroform. The isotropic parameters are $g_{iso} = 1.9864$ and $A_{iso} = (-)74.5$ G.

was recorded on a Varian E-15 spectrometer at room temperature, is characteristic of the hyperfine interaction of the unpaired electron with the ^{51}V nucleus (99.8% abundance, $I = 7/2$). The isotropic EPR parameters calculated from a modified form of the Breit-Rabi equation[13] are $g_{iso} = 1.9864$ and $A_{iso} = (-)74.5$ G.

Single-Crystal X-Ray Data and Data Collection. Suitable crystals for X-ray analysis were grown from chloroform solutions. For $Ti(\eta^5\text{-}C_5H_4CH_3)_2Cl_2$ a dark red crystal with dimensions of 0.35 × 0.35 × 0.35 mm along the [101], [010], and [10$\bar{1}$] directions, respectively, was used to collect the X-ray data. The crystal was mounted on the end of a thin-glass fiber such that the b axis was nearly parallel to the spindle axis of the goniometer. Preliminary oscillation and Weissenberg photographs taken with Cu Kα radiation showed the Laue symmetry to be orthorhombic D_{2h}-$2/m2/m2/m$. Systematic absences for $\{0kl\}$ of $k + l = 2n + 1$ and for $\{hk0\}$ of $h = 2n + 1$ are compatible with two possible space groups, $Pnma$ (D_{2h}^{16}, No. 62) and $Pna2_1$ (C_{2v}^9, No. 33). The former centrosymmetric space group was determined as the correct one by the ultimate structure. For $V(\eta^5\text{-}C_5H_4CH_3)_2Cl_2$ a dark green crystal with dimensions of 0.12 × 0.195 × 0.09 mm along the [100], [010], and [001] directions, respectively, was used for the data collection. This crystal was also mounted such that the b axis was nearly parallel to the spindle axis of the goniometer. Preliminary oscillation and Weissenberg photographs taken with Cu Kα radiation showed the Laue symmetry to be monoclinic C_{2h}-$2/m$. The observed systematic absences for $\{hkl\}$ of $h + k = 2n + 1$ and for $\{h0l\}$ of $l = 2n + 1$ are compatible with two possible space groups, $C2/c$ (C_{2h}^6, No. 15) and Cc (C_s^4, No. 9). The former centrosymmetric space group was determined by the structure ultimately found.

Both crystals were eventually mounted and aligned on a Nova-automated Syntex P$\bar{1}$ diffractometer. The angular coordinates (2θ, ω, ϕ, and χ) of 15 peaks, which were carefully centered with monochromatic Mo Kα radiation ($\lambda(K\alpha_1)$ 0.70926 Å, $\lambda(K\alpha_2)$ 0.71354 Å), were least-squares refined to yield the respective lattice parameters for $Ti(\eta^5\text{-}C_5H_4CH_3)_2Cl_2$ and $V(\eta^5\text{-}C_5H_4CH_3)_2Cl_2$ listed in Table III. The experimental densities were obtained by the flotation method with solutions of carbon tetrachloride and n-heptane.

The fact that there are four formula species per unit cell for both crystal systems indicates that the molecules lie on special positions within the crystal lattices. For $Pnma$, the $Ti(\eta^5\text{-}C_5H_4CH_3)_2Cl_2$ molecules each lie on a mirror plane passing through the titanium and two chlorine atoms. For $C2/c$, the $V(\eta^5\text{-}C_5H_4CH_3)_2Cl_2$ molecules are each constrained to lie along a two-fold rotation axis which bisects the Cl-V-Cl bond angle.

Intensity data were collected for each crystal via the θ-2θ scan mode with a scintillation counter and pulse height analyzer adjusted to admit 90% of the Mo Kα peak. The Bragg 2θ angle for the highly oriented crystal-graphite monochromator was 12.2°, while a takeoff angle of 4° was used for the incident X-ray beam. Variable scan speeds with a minimum of 2.0°/min for $Ti(\eta^5\text{-}C_5H_4CH_3)_2Cl_2$ and 1.0°/min for $V(\eta^5\text{-}C_5H_4CH_3)_2Cl_2$ and variable scan widths based on the overall intensity and width of the peak were employed. A (stationary-crystal)-(stationary-counter) background measurement for one-half of the total scan time was made on each side of a peak. In both cases three standard reflections were periodically measured every 50 reflections to monitor the instrument's stability as well as the crystal's alignment and decay. For $Ti(\eta^5\text{-}C_5H_4CH_3)_2Cl_2$ no significant changes (>3%) in the intensities of these standard reflections were observed. However, for $V(\eta^5\text{-}C_5H_4CH_3)_2Cl_2$ a linear decay correction was made, although the decrease in the intensity of each standard reflection was no greater than 4% during the entire data collection.

Table III. Unit Cell and Space Group Data for $Ti(\eta^5\text{-}C_5H_4CH_3)_2Cl_2$ and $V(\eta^5\text{-}C_5H_4CH_3)_2Cl_2$

	$Ti(\eta^5\text{-}C_5H_4CH_3)_2Cl_2$	$V(\eta^5\text{-}C_5H_4CH_3)_2Cl_2$
System	Orthorhombic	Monoclinic
a, Å	11.928 (5)	13.614 (2)
b, Å	15.147 (6)	6.720 (1)
c, Å	6.848 (4)	13.763 (2)
β, deg	—	105.99 (1)
Volume, Å^3	1237	1210
Density (obsd)	1.50 g/cm^3	1.52 g/cm^3
Density (calcd)	1.503 g/cm^3	1.536 g/cm^3
Z	4	4
μ, cm^{-1}	11.20	12.64
Space group	$Pnma$ (D_{2h}^{16})	$C2/c$ (C_{2h}^6)

For $Ti(\eta^5\text{-}C_5H_4CH_3)_2Cl_2$ all independent reflections corresponding to one octant hkl of the reciprocal lattice were collected for $5° \leq 2\theta \leq 50°$. For $V(\eta^5\text{-}C_5H_4CH_3)_2Cl_2$ two independent octants, hkl and $\bar{h}kl$, of data were restricted to those reflections that are not absent due to C-centering for the range $5° \leq 2\theta \leq 45°$. After correction of the data for background and Lorentz-polarization effects, structure amplitudes were calculated[14] and averaged.[15] The standard deviation for each corrected intensity was obtained from the expression

$$\sigma(I) = (S + B(t_s/t_b)^2 + EI^2)^{1/2}$$

where S designates the total integrated scan count obtained in time t_s, B the total background count obtained in time t_b, E an empirical factor (0.0025), and I the integrated intensity equal to $S - B(t_s/t_b)$. The standard deviation of each structure amplitude, $|F| = (I/Lp)^{1/2}$, was calculated from the expression $\sigma(F) = \sigma(F^2)/2F$. Of the 1136 independent reflections that were sampled for $Ti(\eta^5\text{-}C_5H_4CH_3)_2Cl_2$ only 724 reflections were considered observed with $I > 3\sigma(I)$. For $V(\eta^5\text{-}C_5H_4CH_3)_2Cl_2$ only 590 reflections of the 992 reflections sampled were considered observed with the same criterion.

The linear absorption coefficients, μ, for $Ti(\eta^5\text{-}C_5H_4CH_3)_2Cl_2$ and $V(\eta^5\text{-}C_5H_4CH_3)_2Cl_2$ are 11.20 and 12.64 cm^{-1}, respectively, for Mo Kα radiation. A correction for absorption[16] was made for $Ti(\eta^5\text{-}C_5H_4CH_3)_2Cl_2$ but not for $V(\eta^5\text{-}C_5H_4CH_3)_2Cl_2$ on account of the transmission coefficients calculated for a small set of reflections[17] with widely different orientations varying from 0.62 to 0.76 for $Ti(\eta^5\text{-}C_5H_4CH_3)_2Cl_2$ but only from 0.86 to 0.90 for $V(\eta^5\text{-}C_5H_4CH_3)_2Cl_2$. No corrections for extinction were made.

Single-Crystal EPR Measurements. Dilute single crystals containing ca. 0.2% $V(\eta^5\text{-}C_5H_4CH_3)_2Cl_2$ doped in the host lattice of $Ti(\eta^5\text{-}C_5H_4CH_3)_2Cl_2$ were grown from a chloroform solution in the absence of air. From X-ray photographs the doped crystals were found to possess the same Laue symmetry and cell dimensions as the host material. Because of their sharply defined external morphology shown in Figure 2, the doped crystals could be mounted along the three orthogonal crystallographic axes to within 0.5° without the aid of the X-ray oscillation photographs. The EPR measurements, which were performed on three large crystals, were carried out at room temperature in the same manner as previously described for $V(\eta^5\text{-}C_5H_5)_2S_5$.[5] The line widths observed for $V(\eta^5\text{-}C_5H_4CH_3)_2Cl_2$ were three to five times greater than those observed for $V(\eta^5\text{-}C_5H_5)_2S_5$; a small unresolvable splitting due to a hyperfine interaction with the ^{35}Cl (75.5% abundance, $I = 3/2$) and ^{37}Cl (24.5% abundance, $I = 3/2$) nuclei would increase the observed line widths of the ^{51}V hyperfine components. One eight-line spectrum was obtained for orientations where the direction of the magnetic field is perpendicular to either the a or c axis, while for orientations about the b axis two overlapping eight-line spectra were observed.

Structural Determinations and Refinement of $Ti(\eta^5\text{-}C_5H_4CH_3)_2Cl_2$ and $V(\eta^5\text{-}C_5H_4CH_3)_2Cl_2$. The structures of $Ti(\eta^5\text{-}C_5H_4CH_3)_2Cl_2$ and $V(\eta^5\text{-}C_5H_4CH_3)_2Cl_2$ were both determined by heavy-atom techniques.[18] An interpretation of the three-dimen-

Table IV. Atomic Parameters for $Ti(\eta^5\text{-}C_5H_4CH_3)_2Cl_2$

A. Positional Parameters

Atom	x	y	z
Ti	0.08421 (10)	1/4	0.08466 (16)
Cl(1)	0.13167 (17)	1/4	0.41909 (24)
Cl(2)	0.27357 (18)	1/4	−0.01641 (30)
C(1)	0.0961 (7)	0.4089 (3)	0.1067 (16)
C(2)	−0.0060 (9)	0.3831 (5)	0.1840 (10)
C(3)	−0.0687 (6)	0.3455 (4)	0.0426 (14)
C(4)	−0.0089 (8)	0.3470 (4)	−0.1252 (12)
C(5)	0.0888 (9)	0.3845 (4)	−0.0947 (13)
MeC	0.1799 (8)	0.4564 (6)	0.2284 (20)
H(2)	−0.031	0.390	0.323
H(3)	−0.147	0.321	0.058
H(4)	−0.037 (6)	0.332 (4)	−0.228 (9)
H(5)	0.154 (6)	0.392 (4)	−0.154 (11)

B. Anisotropic Temperature Factors ($\times 10^4$)[a]

Atom	β_{11}	β_{22}	β_{33}	β_{12}	β_{13}	β_{23}
Ti	51 (1)	37 (1)	168 (3)	0[b]	0 (1)	0[b]
Cl(1)	89 (2)	62 (1)	176 (4)	0	−10 (2)	0
Cl(2)	58 (2)	88 (1)	290 (5)	0	32 (3)	0
C(1)	110 (8)	33 (2)	750 (38)	11 (3)	−196 (15)	−17 (7)
C(2)	169 (10)	70 (4)	309 (17)	−58 (5)	−16 (11)	19 (7)
C(3)	66 (6)	62 (3)	559 (29)	−18 (3)	−5 (11)	−18 (8)
C(4)	137 (11)	54 (3)	332 (22)	−11 (5)	−83 (12)	−10 (7)
C(5)	102 (9)	63 (4)	433 (23)	3 (5)	9 (14)	−86 (8)
MeC	256 (15)	68 (5)	1404 (81)	5 (6)	−396 (29)	8 (14)

C. Hydrogen Isotropic Temperature Factors ($Å^2$)

Atom	B
H(2)	8.0
H(3)	8.0
H(4)	7.1 (1.8)
H(5)	6.9 (1.9)

[a] Anisotropic thermal parameters are of the form $\exp[-(\beta_{11}h^2 + \beta_{22}k^2 + \beta_{33}l^2 + 2\beta_{12}hk + 2\beta_{13}hl + 2\beta_{23}kl)]$. [b] β_{12} and β_{23} are required by symmetry to be zero for the atoms lying on a crystallographic mirror plane whose normal is in the b direction; other positional and thermal parameters without esd's were not varied.

sional Patterson map[19] for the $Ti(\eta^5\text{-}C_5H_4CH_3)_2Cl_2$ data yielded initial positions of the titanium and two chlorine atoms on a mirror plane at $y = 1/4$; the coordinates for all nonhydrogen atoms were revealed from subsequent Fourier syntheses.[19] Full-matrix least-squares refinement[20a] with anisotropic temperature factors for the titanium and the two chlorine atoms and with isotropic temperature factors for the carbon atoms resulted in $R_1 = 10.1\%$ and $R_2 = 14.5\%$.[21] A Fourier difference map computed at this point did not resolve the three methyl hydrogen atoms (apparently due to the high thermal motion of the methyl carbon atom of the methylcyclopentadienyl ring) and two of the four cyclopentadienyl hydrogen atoms. Hence, in a further refinement of the nonhydrogen atoms with anisotropic thermal parameters, the coordinates and isotropic thermal parameters of the two resolved ring hydrogen atoms were varied, while the idealized positions of the unresolved hydrogen atoms were calculated before each cycle[22] and then included in the structure factor calculations as fixed-atom contributions. The final full-matrix refinement[20b] reduced R_1 to 4.6% and R_2 to 6.2%. The final goodness-of-fit parameter was 1.66, which indicates a small underestimation in the standard deviation of an observation of unit weight. A final Fourier difference map, which still failed to resolve the methyl hydrogen atoms, revealed no anomalies.[23-26]

Approximate positions of the vanadium atom and the one independent chlorine atom were obtained from an interpretation of a Patterson map;[19] the coordinates for all the nonhydrogen atoms were found from Fourier syntheses. Full-matrix, isotropic least-squares refinement[20a] of this model resulted in $R_1 = 7.7\%$ and $R_2 = 9.3\%$. From a Fourier difference map[19] all four ring hydrogens were located. In addition, one of the three methyl hydrogen atoms was weakly resolved; the positions of the other two methyl hydrogen atoms were calculated with the program MIRAGE.[22] The final least-squares refinement[20b] with anisotropic thermal parameters utilized for all nonhydrogen atoms and isotropic thermal parameters for the ring hydrogens resulted in final discrepancy values of

Table V. Atomic Parameters for $V(\eta^5\text{-}C_5H_4CH_3)_2Cl_2$

A. Positional Parameters

Atom	x	y	z
V	0.0	0.20025 (20)	1/4
Cl	−0.08258 (12)	−0.05846 (25)	0.31825 (12)
C(1)	−0.1408 (5)	0.1575 (9)	0.1073 (5)
C(2)	−0.1667 (6)	0.2886 (14)	0.1744 (6)
C(3)	−0.1067 (7)	0.4582 (12)	0.1830 (6)
C(4)	−0.0416 (6)	0.4322 (10)	0.1223 (5)
C(5)	−0.0635 (6)	0.2512 (11)	0.0750 (5)
MeC	−0.1883 (6)	−0.0370 (12)	0.0684 (6)
H(2)	−0.212 (5)	0.273 (10)	0.201 (5)
H(3)	−0.105 (5)	0.556 (9)	0.222 (5)
H(4)	0.018 (5)	0.540 (11)	0.118 (5)
H(5)	−0.025 (5)	0.205 (11)	0.039 (5)
MeH(1)	−0.226	−0.029	0.000
MeH(2)	−0.138	−0.138	0.074
MeH(3)	−0.233	−0.082	0.105

B. Anisotropic Temperature Factors ($\times 10^4$)

Atom	β_{11}	β_{22}	β_{33}	β_{12}	β_{13}	β_{23}
V	38 (1)	101 (3)	30 (1)	0[a]	7 (1)	0[a]
Cl	59 (1)	195 (4)	54 (1)	−33 (2)	19 (1)	9 (2)
C(1)	53 (5)	153 (16)	47 (5)	−9 (7)	−19 (4)	0 (0)
C(2)	46 (5)	311 (26)	67 (6)	−53 (10)	7 (4)	−17 (11)
C(3)	113 (8)	164 (20)	56 (6)	−70 (11)	−13 (5)	25 (9)
C(4)	89 (6)	176 (19)	44 (5)	19 (9)	−13 (5)	−39 (8)
C(5)	70 (6)	290 (26)	34 (4)	−26 (9)	0 (0)	−19 (8)
MeC	111 (8)	233 (20)	84 (6)	28 (11)	−45 (6)	−23 (10)

C. Hydrogen Isotropic Temperature Factors ($Å^2$)

Atom	B
H(2)	3.9 (1.8)
H(3)	4.0 (1.6)
H(4)	5.8 (1.7)
H(5)	5.9 (2.1)
MeH(1)	8.0
MeH(2)	8.0
MeH(3)	8.0

[a] For the vanadium atom located on a crystallographic twofold rotation axis in the b direction, β_{12} and β_{23} are required by symmetry to be zero; positional and thermal parameters without esd's were not varied.

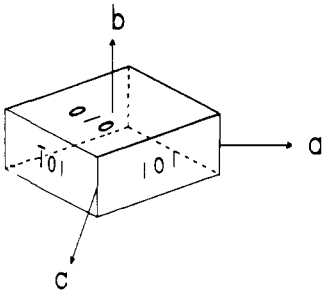

Figure 2. External crystal morphology of $Ti(\eta^5\text{-}C_5H_4CH_3)_2Cl_2$ used as the host crystal lattice in the single-crystal EPR measurements of $V(\eta^5\text{-}C_5H_4CH_3)_2Cl_2$.

$R_1 = 4.1\%$ and $R_2 = 4.8\%$. The goodness-of-fit parameter was 1.08. The isotropic thermal parameter for each of the methyl hydrogens was fixed at 8.0 $Å^2$. A final Fourier difference map revealed no residual electron density greater than 0.2 e/$Å^3$.[23-26]

The positional and thermal parameters for $Ti(\eta^5\text{-}C_5H_4CH_3)_2Cl_2$ and for $V(\eta^5\text{-}C_5H_4CH_3)_2Cl_2$, obtained from the output of the final least-squares cycle, are presented in Tables IV and V, respectively.[27] Interatomic distances and angles with estimated standard deviations, calculated from the variance-covariance matrix,[28] are provided in Table VI for $Ti(\eta^5\text{-}C_5H_4CH_3)_2Cl_2$ and $V(\eta^5\text{-}C_5H_4CH_3)_2Cl_2$. The "best" least-squares planes[29] defined by specified atoms along with the perpendicular distances of these and other atoms from these planes and the angles between the normals to these planes are presented in Table VII for $Ti(\eta^5\text{-}C_5H_4CH_3)_2Cl_2$ and $V(\eta^5\text{-}C_5H_4CH_3)_2Cl_2$.

Table VI. Interatomic Distances (Å) and Angles (deg) for $Ti(\eta^5\text{-}C_5H_4CH_3)_2Cl_2$ and $V(\eta^5\text{-}C_5H_4CH_3)_2Cl_2$

A. Bond Distances

	$Ti(\eta^5\text{-}C_5H_4CH_3)_2Cl_2$ (M = Ti)	$V(\eta^5\text{-}C_5H_4CH_3)_2Cl_2$ (M = V)		$Ti(\eta^5\text{-}C_5H_4CH_3)_2Cl_2$ (M = Ti)	$V(\eta^5\text{-}C_5H_4CH_3)_2Cl_2$ (M = V)
M–Cl(1)	2.359 (2)	2.398 (2)	C(2)–C(3)	1.350 (10)	1.388 (11)
M–Cl(2)	2.362 (2)		C(4)–C(5)	1.313 (11)	1.373 (10)
	2.361 (av)			1.332 (av)	1.381 (av)
M–C(1)	2.354 (6)	2.416 (5)	C(3)–C(4)	1.352 (10)	1.385 (11)
M–C(2)	2.298 (7)	2.385 (6)	C(2)–H(2)	1.00	0.81 (6)
M–C(5)	2.349 (6)	2.380 (6)	C(3)–H(3)	1.00	0.85 (6)
	2.324 (av)	2.383 (av)	C(4)–H(4)	0.81 (7)	1.10 (7)
M–C(3)	2.286 (7)	2.345 (6)	C(5)–H(5)	0.89 (7)	0.87 (7)
M–C(4)	2.300 (6)	2.336 (6)		0.93 (av)	0.91 (av)
	2.293 (av)	2.341 (av)	MeC–MeH(1)	—[a]	0.94
C(1)–MeC	1.487 (10)	1.491 (9)	MeC–MeH(2)	—	0.95
			MeC–MeH(3)	—	0.94
C(1)–C(2)	1.384 (11)	1.390 (10)			0.94 (av)
C(1)–C(5)	1.430 (11)	1.400 (9)	M–Cp(c)[b]	2.067	1.991
	1.407 (av)	1.395 (av)	Cp(c) · · · Cp'(c)[c]	3.750	3.657

B. Bond Angles

	(M = Ti)	(M = V)		(M = Ti)	(M = V)
Cl(1)–M–Cl(2)	93.15 (8)	87.06 (9)	C(2)–C(3)–C(4)	108.1 (7)	107.7 (7)
Cp(c)–M–Cp(c)'	130.2	133.4	C(3)–C(4)–C(5)	109.9 (7)	107.9 (7)
				109.0 (av)	107.8 (av)
Cp(c)–M–Cl(1)	106.6	107.4	C(2)–C(1)–MeC	120.9 (1.1)	129.0 (8)
Cp(c)–M–Cl(2)	107.0	105.9	C(5)–C(1)–MeC	134.9 (1.1)	124.8 (7)
	106.8 (av)	106.7 (av)		127.9 (av)	126.9 (av)
C(5)–C(1)–C(2)	104.0 (7)	106.0 (6)	C(1)–MeC–MeH(1)	—	111.9
C(1)–C(2)–C(3)	109.4 (7)	109.0 (7)	C(1)–MeC–MeH(2)	—	111.2
C(4)–C(5)–C(1)	108.6 (8)	109.3 (7)	C(1)–MeC–MeH(3)	—	111.8
	109.0 (av)	109.2 (av)			

C. Nonbonded Intramolecular Contacts Less than 4.0 Å about the Central Metal Atom and the Chlorine Atom(s)[d]

	(M = Ti)		(M = V)		(M = Ti)		(M = V)
M · · · MeC	3.437		3.439	Cl(1) · · · C(2)	3.058	Cl · · · C(2)	3.069
M · · · H(1)	3.008		2.822	Cl(1) · · · C(3)	3.801	Cl · · · C(3)	3.910
M · · · H(2)	2.961		2.757	Cl(1) · · · H(2)	2.950	Cl · · · H(2)	3.015
M · · · H(3)	2.862		2.963	Cl(1) · · · MeH(2)	—	Cl · · · MeH(2)	3.284
M · · · H(4)	2.830		2.825	Cl(1) · · · MeH(3)	—	Cl · · · MeH(3)	3.087
M · · · MeH(2)	—[a]		3.472	Cl(2) · · · C(1)	3.315	Cl' · · · C(1)	3.269
M · · · MeH(3)	—		3.765	Cl(2) · · · C(4)	3.751	Cl' · · · C(4)	3.693
Cl(1) · · · MeC	3.437	Cl · · · MeC	3.345	Cl(2) · · · C(5)	3.049	Cl' · · · C(5)	2.972
Cl(2) · · · MeC	3.720	Cl' · · · MeC	3.589	Cl(2) · · · H(5)	2.748	Cl' · · · H(5)	2.745
Cl(1) · · · Cl(2)	3.429	Cl · · · Cl'	3.303	Cl(2) · · · MeH(2)	—	Cl' · · · MeH(2)	3.006
Cl(1) · · · C(1)	3.248	Cl · · · C(1)	3.146				

D. Other Nonbonded Intramolecular Contacts Less than 2.5 Å

H(3)–H'(3)	2.15	H(3)–H'(4)	2.19
H(4)–H'(4)	2.48	H(4)–H'(3)	2.19
		MeH–MeH	1.54

[a] The methyl hydrogen atoms were not located in the titanium complex. [b] Cp(c) designates the centroid of a cyclopentadienyl ring. [c] For $Ti(\eta^5\text{-}C_5H_4CH_3)_2Cl_2$ and for $V(\eta^5\text{-}C_5H_4CH_3)_2Cl_2$ the position of the symmetry related (primed) atom is determined by a substitution of the position of the corresponding (nonprimed) atom into the relationships $x, \frac{1}{2} - y, z$ and $-x, y, \frac{1}{2} - z$, respectively. [d] No intermolecular contacts less than 2.8 and 2.7 Å about any of the atoms were found for $Ti(\eta^5\text{-}C_5H_4CH_3)_2Cl_2$ and $V(\eta^5\text{-}C_5H_4CH_3)_2Cl_2$, respectively.

Results and Discussion

General Description of the Molecular and Crystal Structures. The molecular structures of $Ti(\eta^5\text{-}C_5H_4CH_3)_2Cl_2$ and $V(\eta^5\text{-}C_5H_4CH_3)_2Cl_2$ which are shown in Figures 3a and 3b,[30] respectively, are essentially identical except for a variation in the orientation of the methyl group. The two chlorine atoms and centroids of the two methylcyclopentadienyl rings formally occupy four tetrahedral-like coordination sites about the central metal atom. With the assumption of cylindrical symmetry for the pentahaptocoordinated methylcyclopentadienyl rings, the ligand arrangement about the metal atoms in both cases conforms closely to C_{2v}-$2mm$ symmetry. Each molecule of $Ti(\eta^5\text{-}C_5H_4CH_3)_2Cl_2$ lies on a crystallographic mirror plane, whereas each molecule of $V(\eta^5\text{-}C_5H_4CH_3)_2Cl_2$ possesses a crystallographic twofold axis. The crystalline arrangement of the $Ti(\eta^5\text{-}C_5H_4CH_3)_2Cl_2$ molecules in the orthorhombic unit cell of *Pnma* symmetry is depicted in a [001] projection shown in Figure 4a. The corresponding disposition of the $V(\eta^5\text{-}C_5H_4CH_3)_2Cl_2$ molecules in the monoclinic unit cell of $C2/c$ symmetry is illustrated in a [001] projection given in Figure 4b. These diagrams emphasize that the crystal packing of the four $V(\eta^5\text{-}C_5H_4CH_3)_2Cl_2$ molecules in the unit cell is entirely different from that for the titanium analog.

Discussion of X-Ray Results. The structural analysis of $Ti(\eta^5\text{-}C_5H_5)_2Cl_2$ has been hindered by the fact that crystals obtained from most solvents are invariably twinned. However, Clearfield, Bernal, and coworkers[8] recently isolated

Table VII. Least-Squares Molecular Planes for $Ti(\eta^5\text{-}C_5H_4CH_3)_2Cl_2$ and $V(\eta^5\text{-}C_5H_4CH_3)_2Cl_2$

I. Equations of Least-Squares Planes and Perpendicular Distances (Å) of Atoms to These Planes

A. $Ti(\eta^5\text{-}C_5H_4CH_3)_2Cl_2$[a,c]

1. Plane through Ti, Cl(1), and Cl(2)

$-0.0000X + 1.0000Y - 0.0000Z - 3.7868 = 0$

C(1)	2.41	C(5)	2.07	H(4)	1.25
C(2)	2.02	MeC	3.13	H(5)	2.14
C(3)	1.45	H(2)	2.13		
C(4)	1.47	H(3)	1.08		

2. Plane through C(1), C(2), C(3), C(4), and C(5)

$-0.3900X + 0.8938Y - 0.2216Z - 4.9321 = 0$

C(1)	−0.005	Ti	−2.07	H(3)	−0.01
C(2)	0.003	Cl(1)	−2.80	H(4)	0.09
C(3)	0.000	Cl(2)	−2.80	H(5)	−0.12
C(4)	−0.003	MeC	0.06		
C(5)	0.005	H(2)	0.01		

3. Plane through Ti, Midpoint between Cl(1) and Cl(2), Cp(c), and Cp'(c)

$0.4883X - 0.0000Y - 0.8727Z + 0.0210 = 0$

Ti	0.006	C(1)	−0.06	MeC	−0.30
Cp(c)	−0.002	C(2)	−1.11	H(2)	−2.08
Cp'(c)	−0.002	C(3)	−0.63	H(3)	−1.18
Cl(1)	−1.72	C(4)	0.72	H(4)	1.17
Cl(2)	1.71	C(5)	1.10	H(5)	1.84

4. Plane through C'(1), C'(2), C'(3), C'(4), and C'(5)

$-0.3900X - 0.8938Y - 0.2216Z + 1.8370 = 0$

B. $V(\eta^5\text{-}C_5H_4CH_3)_2Cl_2$[b,c]

1. Plane through V, Cl, and Cl'

$-0.5467X + 0.0000Y - 0.8373Z + 2.2512 = 0$

C(1)	2.33	MeC	3.04	H(5)	2.08
C(2)	1.92	H(2)	2.02	MeH(1)	3.93
C(3)	1.40	H(3)	1.03	MeH(2)	2.61
C(4)	1.46	H(4)	1.05	MeH(3)	3.04
C(5)	2.05				

2. Plane through C(1), C(2), C(3), C(4), and C(5)

$-0.4944X + 0.4245Y - 0.7585Z - 0.5244 = 0$

C(1)	−0.003	V	−1.99	H(4)	−0.07
C(2)	−0.003	Cl	−2.73	H(5)	−0.09
C(3)	−0.003	MeC	0.08	MeH(1)	0.91
C(4)	0.007	H(2)	0.04	MeH(2)	−0.59
C(5)	−0.009	H(3)	−0.05	MeH(3)	−0.05

3. Plane through V, Midpoint between Cl and Cl', Cp(c) and Cp'(c)

$0.8479X - 0.0000Y - 0.5301Z - 2.5572 = 0$

V	0.000	C(4)	0.83	H(5)	1.87
Cp(c)	0.000	C(5)	1.06	MeH(1)	−0.04
Cl	−1.65	MeC	−0.32	MeH(2)	0.21
C(1)	−0.17	H(2)	−1.95	MeH(3)	−1.21
C(2)	−1.15	H(3)	−0.93		
C(3)	−0.55	H(4)	1.55		

4. Plane through C'(1), C'(2), C'(3), C'(4), and C'(5)

$-0.4944X - 0.4245Y - 0.7585Z - 4.6048 = 0$

II. Angles (deg) between Normals to Planes

A. $Ti(\eta^5\text{-}C_5H_4CH_3)_2Cl_2$

1 and 2	26.6	2 and 3	89.8
1 and 3	90.0	2 and 4	53.3
1 and 4	26.6	3 and 4	89.8

B. $V(\eta^5\text{-}C_5H_4CH_3)_2Cl_2$

1 and 2	25.1	2 and 3	91.0
1 and 3	91.1	2 and 4	50.2
1 and 4	25.1	3 and 4	91.0

[a] The equations of the planes are given in orthogonal angström coordinates (X, Y, Z) which are related to the fractional unit cell coordinates (x, y, z) as follows: $X = ax$, $Y = by$, $Z = cz$. [b] The equations of the planes are given in orthogonal angström coordinates (X, Y, Z) which are related to the fractional unit cell coordinates (x, y, z) as follows: $X = ax + cz \cos\beta$, $Y = by$, $Z = cz \sin\beta$. [c] Unit weights were used for all atoms in all plane calculations.

untwinned crystals of $Ti(\eta^5\text{-}C_5H_5)_2Cl_2$ from hot benzene and carried out a X-ray structural determination. A comparison of their results[31] with those of $Ti(\eta^5\text{-}C_5H_4CH_3)_2Cl_2$

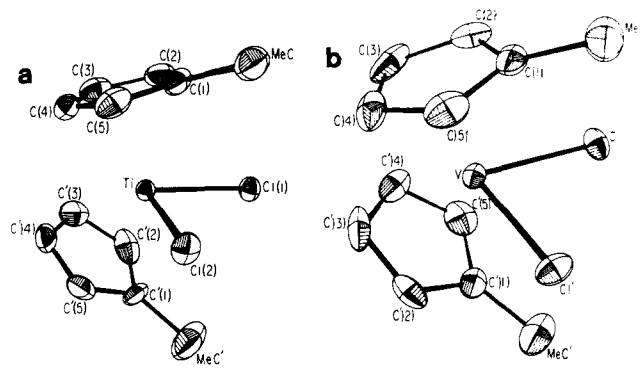

Figure 3. Molecular view of (a) $Ti(\eta^5\text{-}C_5H_4CH_3)_2Cl_2$ with 20% probability thermal ellipsoids and (b) $V(\eta^5\text{-}C_5H_4CH_3)_2Cl_2$ with 30% probability thermal ellipsoids. Primed atoms are related to unprimed atoms by a mirror plane and a twofold rotation axis for $Ti(\eta^5\text{-}C_5H_4CH_3)_2Cl_2$ and $V(\eta^5\text{-}C_5H_4CH_3)_2Cl_2$, respectively.

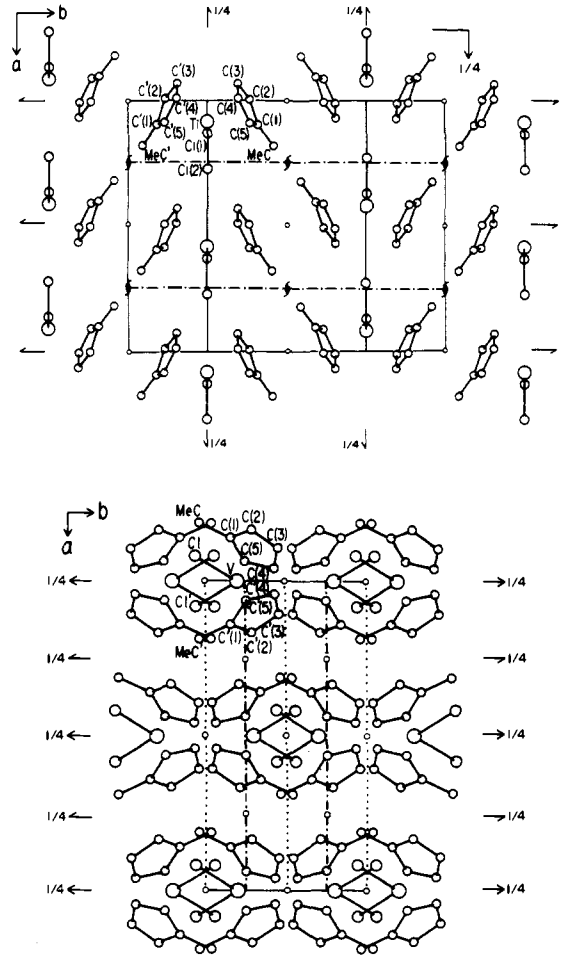

Figure 4. (Top) [001] unit cell projection of the $Ti(\eta^5\text{-}C_5H_4CH_3)_2Cl_2$ molecules in the orthorhombic unit cell of *Pnma* symmetry; (bottom) [001] unit cell projection of the $V(\eta^5\text{-}C_5H_4CH_3)_2Cl_2$ molecules in the monoclinic unit cell of $C2/c$ symmetry.

demonstrates that the substitution of the methyl group on each cyclopentadienyl ring has an essentially negligible effect on the basic molecular configuration in that the corresponding bond distances and angles differ by less than 0.01 Å and 1.3°, respectively.

The thermal motion determined in $Ti(\eta^5\text{-}C_5H_4CH_3)_2Cl_2$ is generally greater than that in $V(\eta^5\text{-}C_5H_4CH_3)_2Cl_2$; this difference can be rationalized on the basis of the lower density (arising from a larger volume of the unit cell) for $Ti(\eta^5\text{-}C_5H_4CH_3)_2Cl_2$ due to the looser crystal packing of the $Ti(\eta^5\text{-}$

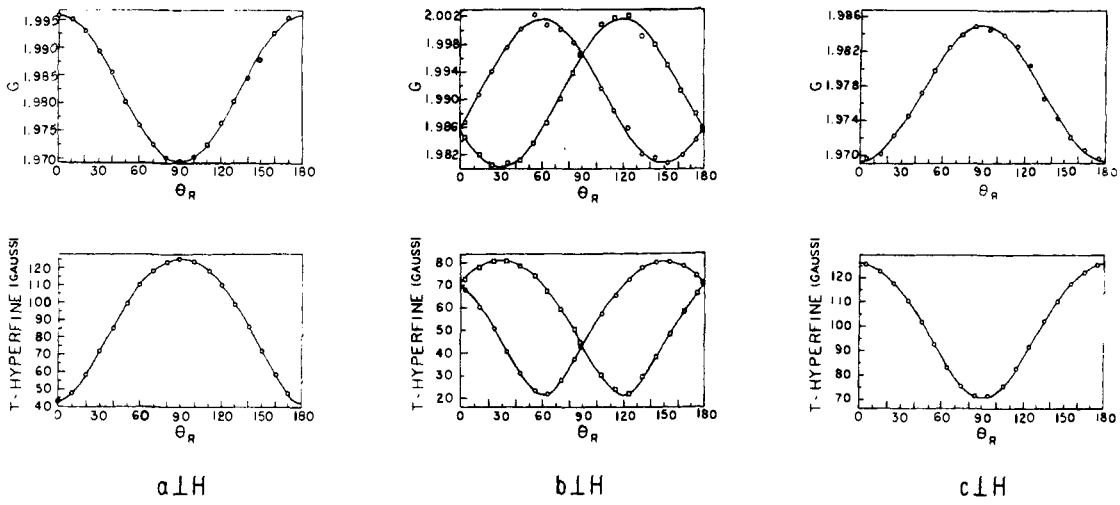

Figure 5. Plots of the experimental g value and hyperfine coupling constant, T, vs. the angle of rotation, θ_R, for each of the three orthogonal sets of EPR data obtained for $V(\eta^5\text{-}C_5H_4CH_3)_2Cl_2$ diluted in the crystal lattice of $Ti(\eta^5\text{-}C_5H_4CH_3)_2Cl_2$. The solid lines represents the best fit of the experimental data (open symbols) to a three-parameter equation, $P\cos^2\theta_i + Q\sin^2\theta_i - 2R\sin\theta_i\cos\theta_i$.

$C_5H_4CH_3)_2Cl_2$ molecules in the unit cell. On account of the relatively large anisotropic thermal parameters for the cyclopentadienyl carbon atoms in the titanium complex, especially for the methyl carbon atom in the plane of the methylcyclopentadienyl ring, the positions of the three methyl hydrogen atoms and two of the ring hydrogen atoms could not be resolved. This much greater thermal motion is also reflected in the C-C bond-length range for $Ti(\eta^5\text{-}C_5H_4CH_3)_2Cl_2$ of 1.31 (1) to 1.43 (1) Å being considerably greater than the corresponding range for $V(\eta^5\text{-}C_5H_4CH_3)_2Cl_2$ of 1.37 (1) to 1.40 (1) Å. The C-C bond distances for $V(\eta^5\text{-}C_5H_4CH_3)_2Cl_2$ are comparable to those obtained for the cyclopentadienyl rings in $Ti(\eta^5\text{-}C_5H_5)_2Cl_2$[8] and (1,1′-trimethylenedicyclopentadienyl)titanium dichloride.[32]

The most evident difference between $Ti(\eta^5\text{-}C_5H_4CH_3)_2Cl_2$ and $V(\eta^5\text{-}C_5H_4CH_3)_2Cl_2$ is the Cl-M-Cl bond angle. The Cl-V-Cl bond angle of 87.1 (1)° is ca. 6° *smaller* than the Cl-Ti-Cl bond angle of 93.2 (1)°. This result, which is consistent with those obtained from similar comparisons of the S-M-S bond angles between $Ti(\eta^5\text{-}C_5H_5)_2(SC_6H_5)_2$[2a,b] and $V(\eta^5\text{-}C_5H_5)_2(SC_6H_5)_2$[2a,b] and between $Ti(\eta^5\text{-}C_5H_5)_2S_5$[2a,c,33] and $V(\eta^5\text{-}C_5H_5)_2S_5$,[2a,c] provides further structural evidence for the breakdown of the Ballhausen-Dahl bonding model for $M(\eta^5\text{-}C_5H_5)_2L_2$-type complexes. The nonbonding Cl—Cl contacts for $Ti(\eta^5\text{-}C_5H_4CH_3)_2Cl_2$ and $V(\eta^5\text{-}C_5H_4CH_3)_2Cl_2$ of 3.429 and 3.303 Å, respectively, are less than twice the van der Waals radius of 1.8 Å for a chlorine atom.[34]

Another prominent structural difference between $Ti(\eta^5\text{-}C_5H_4CH_3)_2Cl_2$ and $V(\eta^5\text{-}C_5H_4CH_3)_2Cl_2$ is the 0.08 Å shorter V-Cp(c) distance (Table VI) which can be readily attributed to the smaller covalent radius of vanadium (viz., 1.22 Å) compared to that for titanium (viz., 1.32 Å).[34] This significant shortening of the V-Cp(c) distance compared to the Ti-Cp(c) distance is consistent with the trend observed for other bis(cyclopentadienyl)titanium and vanadium complexes.[2]

The Cp(c)-M-Cp′(c) angles of 129.9 and 133.4° for $Ti(\eta^5\text{-}C_5H_4CH_3)_2Cl_2$ and $V(\eta^5\text{-}C_5H_4CH_3)_2Cl_2$, respectively, fall within the range of 130-135° found for other $M(\eta^5\text{-}C_5H_5)_2L_2$-type complexes. These values indicate that the mode of bonding of the rings to the metal atom is essentially invariant to the substitution of one methyl group on each of the rings. The H_3C-C bond lengths in $Ti(\eta^5\text{-}C_5H_4CH_3)_2Cl_2$ and $V(\eta^5\text{-}C_5H_4CH_3)_2Cl_2$ have an identical value of 1.49 (1) Å which is in the expected range for a $C(sp^3)$-$C(sp^2)$ bond length.

On the basis of covalent-radii arguments, it would be expected that the Ti-Cl bond distance should be ca. 0.10 Å longer than the V-Cl distance. However, the two independent Ti-Cl bond lengths in $Ti(\eta^5\text{-}C_5H_4CH_3)_2Cl_2$ of 2.359 (2) and 2.362 (2) Å are 0.04 Å *shorter* than the one independent V-Cl bond length of 2.398 (2) Å in $V(\eta^5\text{-}C_5H_4CH_3)_2Cl_2$. This reversed trend for the M-L bond lengths (from that found for the M-Cp(c) distances), which also was observed between $Ti(\eta^5\text{-}C_5H_5)_2(SC_6H_5)_2$ and $V(\eta^5\text{-}C_5H_5)_2(SC_6H_5)_2$ and between $Ti(\eta^5\text{-}C_5H_5)_2S_5$ and $V(\eta^5\text{-}C_5H_5)_2S_5$, may be rationalized on the basis of composite effects—one being due to increased nonbonding intramolecular repulsive forces resulting from the shorter M-Cp(c) distance in the V(IV) complexes and the other being a consequence of the unpaired electron in each V(IV) complex occupying a MO which is antibonding with respect to the V-L bonds.

The close Cl—Cl nonbonding contacts, especially in $V(\eta^5\text{-}C_5H_4CH_3)_2Cl_2$, along with the possible antibonding effect of the unpaired electron on the chlorine ligands suggests that both the size and nature of the ligand L in $V(\eta^5\text{-}C_5H_5)_2L_2$ complexes are important factors in determining the stability of these complexes. While the $Ti(\eta^5\text{-}C_5H_5)_2X_2$ (X = Cl, Br, I) complexes are easily isolatable and readily sublimable, the corresponding vanadium complexes are not. In fact, of the three vanadium complexes only the chloride complex is thermally stable at room temperature.

Results of Dilute Single-Crystal EPR Investigation. The EPR spectra obtained for single crystals of $V(\eta^5\text{-}C_5H_4CH_3)_2Cl_2$ doped in the crystal lattice of $Ti(\eta^5\text{-}C_5H_4CH_3)_2Cl_2$ were analyzed in the same manner as the spectral data obtained for $V(\eta^5\text{-}C_5H_5)_2S_5$.[5] The components of the g^2 and K^2 matrices (Table III) for the two nonequivalent magnetic sites of the $V(\eta^5\text{-}C_5H_4CH_3)_2Cl_2$ molecules were determined from a least-squares fit of the experimental data to the three-parameter equation

$$y_i = P\cos^2\theta_i + Q\sin^2\theta_i - 2R\sin\theta_i\cos\theta_i$$

where $y_i = g^2$ or g^2T^2. Figure 5 shows plots of the experimental g values and the corresponding hyperfine coupling constants vs. the angle of rotation for each of the three orthogonal sets of EPR data.

Unlike the case of $V(\eta^5\text{-}C_5H_5)_2S_5$, the Eulerian angles

Table VIII. Final Analysis of Single-Crystal EPR Data Obtained for the Two Magnetically Nonequivalent $V(\eta^5\text{-}C_5H_4CH_3)_2Cl_2$ Molecules Doped in the Diamagnetic $Ti(\eta^5\text{-}C_5H_4CH_3)_2Cl_2$ Host[a]

	Molecule 1		Molecule 2	
	g^2	K^2	g^2	K^2
P_a	3.98329	7287.72	3.98329	7287.72
Q_a	3.87910	60995.5	3.87910	60995.5
R_a	−0.000249	16.2369	−0.000249	16.2369
σ_g	0.00022		0.00022	
σ_T	0.38		0.38	
P_b	3.94402	19850.4	3.94259	19858.1
Q_b	3.98602	7563.01	3.98546	7717.29
R_b	−0.034978	10145.1	0.037088	−10224.3
σ_g	0.00048		0.00052	
σ_T	0.40		0.38	
P_c	3.87871	61137.0	3.87871	61137.0
Q_c	3.94032	19558.4	3.94032	19558.4
R_c	−0.000246	27.8389	−0.000246	27.8389
σ_g	0.00030		0.00030	
σ_T	0.27		0.27	
g_x	1.9805		1.9799	
g_y	1.9695		1.9694	
g_z	2.0011		2.0014	
g_{av}	1.9837		1.9836	
ϕ	−89.91		89.69	
θ	150.70		−29.97	
Ψ	−89.48		−89.86	
T_x	(−)80.5 G		(−)80.7 G	
T_y	(−)125.5 G		(−)125.5 G	
T_z	(−)20.6 G		(−)20.6 G	
T_{av}	(−)75.5 G		(−)75.6 G	
ϕ	−90.00		89.94	
θ	150.59		−29.59	
Ψ	−89.94		−89.98	

[a] The estimated standard deviations, σ_g and σ_T, were calculated from $\sigma_g = [\Sigma_{i=1}(g_{calcd} - g_{exptl})^2/(n-1)]^{1/2}$ and $\sigma_T = [\Sigma_{i=1}(T_{calcd} - T_{exptl})^2/(n-1)]^{1/2}$ for each least-squares curve with n observations.

(Φ, θ, Ψ)[35] given in Table VIII demonstrate that the principal axes of the **g** and **T** tensors are coincident for $V(\eta^5\text{-}C_5H_4CH_3)_2Cl_2$, which is consistent with the fact that the dilute powder EPR spectra of $V(\eta^5\text{-}C_5H_4CH_3)_2Cl_2$ (Figure 6) were simulated[36a,b] from a second-order expression[36c] derived on the basis of their coincidence. Since each $V(\eta^5\text{-}C_5H_4CH_3)_2Cl_2$ molecule in the host lattice of $Ti(\eta^5\text{-}C_5H_4CH_3)_2Cl_2$ lies on a mirror plane, the orientation of the principal directions of **g** and **T** can be visualized in Figure 7, which corresponds to a projection of the contents of the host lattice along the [010] direction. Since only *one* eight-line spectrum is observed for orientations of the two nonequivalent magnetic sites with either the *a* or *c* axis perpendicular to the direction of the magnetic field, the *y* component of **g** and **T** must be normal to the mirror plane containing the vanadium and two chlorine atoms; the *x* and *z* components are constrained to lie within this plane. The actual orientation of the principal directions for the magnetic tensors with respect to the molecular geometry of $V(\eta^5\text{-}C_5H_4CH_3)_2Cl_2$ is depicted in Figure 8. The orientation of the **g** and **T** tensors for $V(\eta^5\text{-}C_5H_4CH_3)_2Cl_2$ is identical with the orientation of the principal directions found for the **T** tensor for $V(\eta^5\text{-}C_5H_5)_2S_5$. The direction of the *x* component bisects the Cl-V-Cl bond angle, the *y* component is normal to the plane containing the vanadium and two chlorine ligands, and the *z* component is normal to the plane which bisects the Cl-V-Cl bond angle.

The coincidence of the principal directions of **g** and **T** for $V(\eta^5\text{-}C_5H_4CH_3)_2Cl_2$ not only reflects its higher molecular symmetry (in comparison to that of $V(\eta^5\text{-}C_5H_5)_2S_5$) but also demonstrates that the principal axial systems for **g** and

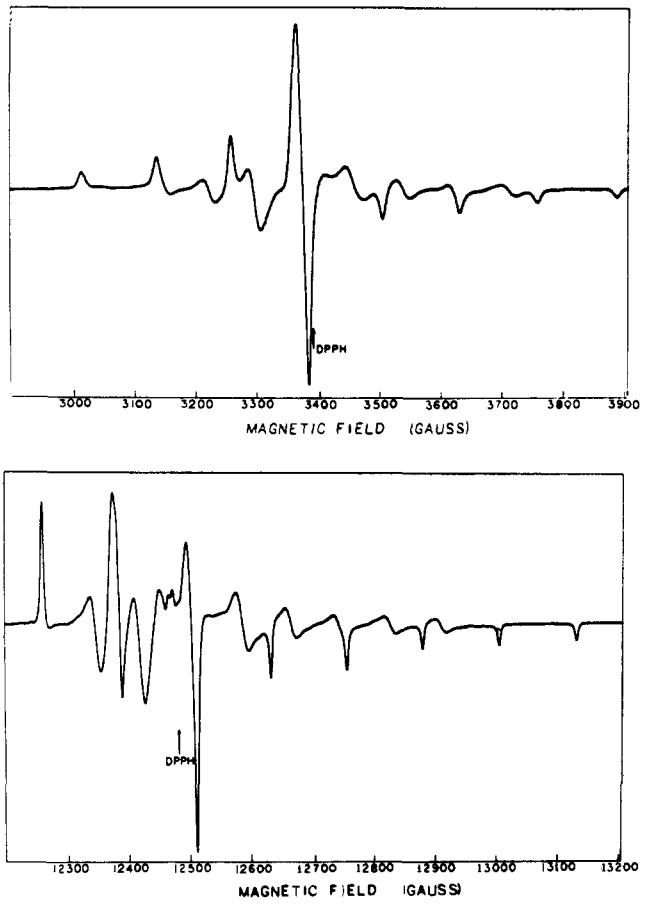

Figure 6. Powder EPR spectra recorded at room temperature for $V(\eta^5\text{-}C_5H_4CH_3)_2Cl_2$ diluted in $Ti(\eta^5\text{-}C_5H_4CH_3)_2Cl_2$: (top) X-band, ν_0 = 9.5216 GHz; and (bottom) Q-band, ν_0 = 35.004 GHz.

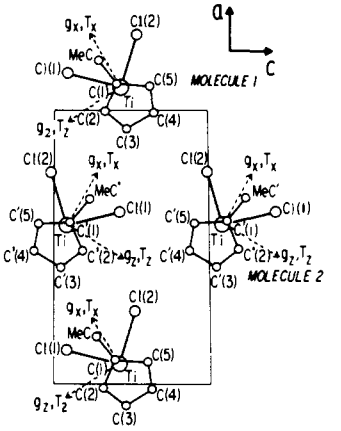

Figure 7. The [010] projection of the host lattice $Ti(\eta^5\text{-}C_5H_4CH_3)_2Cl_2$. The principal directions of the *x* and *z* components of the **g** and **T** tensors for $V(\eta^5\text{-}C_5H_4CH_3)_2Cl_2$ (represented by dashed arrows) are included to illustrate the two nonequivalent sites.

T are strongly dependent on the molecular symmetry. On the other hand, the fact that the principal axes of **T** for $V(\eta^5\text{-}C_5H_5)_2S_5$ and $V(\eta^5\text{-}C_5H_4CH_3)_2Cl_2$ are identical supports the premise that the directional properties of the metal components of the molecular orbital containing the unpaired electron are apparently invariant to the type of ligand L.

The average principal values of the **g** and **T** tensors for the two nonequivalent magnetic sites of $V(\eta^5\text{-}C_5H_4CH_3)_2Cl_2$ are given in Table IX. Based on the same li-

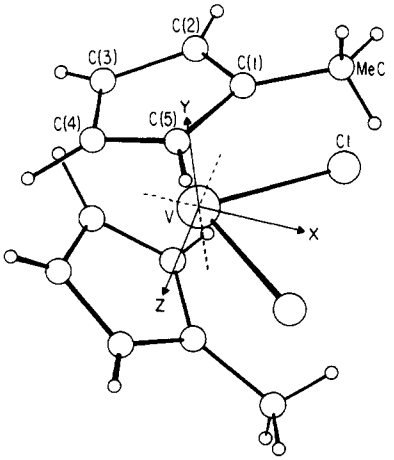

Figure 8. Orientation of the principal axes for the magnetic tensors with respect to the molecular geometry of $V(\eta^5\text{-}C_5H_4CH_3)_2Cl_2$.

Table IX. Experimental g and T Tensors with Best-Fit Parameters (av) from Single-Crystal EPR Study of $V(\eta^5\text{-}C_5H_4CH_3)_2Cl_2$ Doped in $Ti(\eta^5\text{-}C_5H_4CH_3)_2Cl_2$

$g_x = 1.9802$	$\phi = -89.91$
$g_y = 1.9695$	$\theta = 150.35$
$g_z = 2.0013$	$\psi = -89.47$
$T_x = (-)80.6$ G	$\phi = -90.00$
$T_y = (-)125.5$ G	$\theta = 150.50$
$T_z = (-)20.6$ G	$\Psi = -89.94$

For $a = -0.976$ and $b = 0.218$, where $|\Psi_0\rangle = a|d_{z^2}\rangle + b|d_{x^2-y^2}\rangle$

$T_x = (-)80.8$ G	$P = 97.0 \times 10^{-4}$ cm^{-1}
$T_y = (-)125.4$ G	$\langle r^{-3}\rangle = 2.07$ au
$T_z = (-)20.5$ G	$\chi = -2.21$
$K = 68.8 \times 10^{-4}$ cm^{-1}	$\lambda = 61$ cm^{-1}

$\Delta E_{xz} = 11973$ cm^{-1}
$\Delta E_{yz} = 13544$ cm^{-1}
$\Delta E_{xy} = 23142$ cm^{-1}

per cent character of $3d_{z^2}$ to $3d_{x^2-y^2}$, $a^2/b^2 = (-0.976)/(0.218)^2 = 20.0/1$

gand-field model previously employed[5] to interpret the single-crystal EPR data for $V(\eta^5\text{-}C_5H_5)_2S_5$, the metal orbital character of the unpaired electron as well as the corresponding EPR parameters (i.e., χ, P, K, $\langle r^{-3}\rangle$, and λ) have been calculated from the principal components of the hyperfine coupling tensor. The "best" values of the mixing coefficients, a and b, for the electronic ground state, $|\Psi_0\rangle = a|d_{z^2}\rangle + b|d_{x^2-y^2}\rangle$ reveal that the anisotropy in the hyperfine coupling interaction arises primarily from the significantly different character of the $3d_{z^2}$ and $3d_{x^2-y^2}$ AO's. The closeness of the a^2/b^2 ratio of $(-0.976)^2/(0.218)^2 = 20.0/1$ for $V(\eta^5\text{-}C_5H_4CH_3)_2Cl_2$ compared to that of $(-0.963)^2/(0.270)^2 = 12.7/1$ for $V(\eta^5\text{-}C_5H_5)_2S_5$ substantiates the correctness of our interpretation of the EPR data of $V(\eta^5\text{-}C_5H_5)_2S_5$ concerning the distribution of the unpaired electron.

The actual values calculated for the mixing coefficients, a and b, are dependent upon the choice of the master coordinate system, and consequently the a^2/b^2 ratio is not rotationally invariant. To demonstrate this more clearly, the values of a and b in Table IX were transformed to a right-handed Cartesian coordinate system which differs from that for the principal directions of **T** by a simple permutation of axial labels (i.e., x becomes z', y becomes x', and z becomes y'). The necessary transformation for the d_{z^2} and $d_{x^2-y^2}$ AO's is $d_{z'^2} = -0.500d_{z^2} + 0.866d_{x^2-y^2}$ and $d_{x'^2-y'^2} = -0.866d_{z^2} - 0.500d_{x^2-y^2}$. In the (x', y', z') system the mixing coefficients become $a' = 0.677$ and $b' = 0.736$, which indicates that the $3d_{z'^2}$ and $3d_{x'^2-y'^2}$ orbitals contribute almost equally (i.e., $a'^2/b'^2 \simeq 1$) to the metal composition of the molecular orbital.

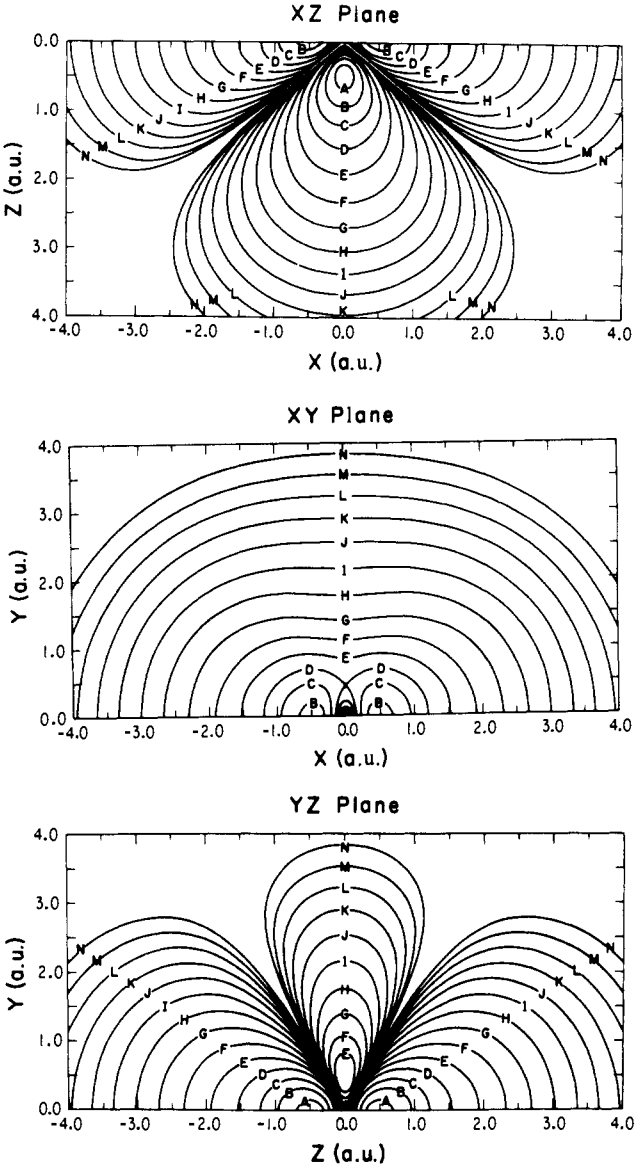

Figure 9. Electron-density contour map of $|\Psi_0\rangle = -0.976d_{z^2} + 0.218 d_{x^2-y^2}$ for (top) xz plane, (middle) xy plane, and (bottom) yz plane. These three principal sections show the anisotropy of the relative density distribution of the unpaired electron localized on the vanadium atom in $V(\eta^5\text{-}C_5H_4CH_3)_2Cl_2$. The coordinates in atomic units for the vanadium atom are 0,0,0 and for the two chlorine atoms are 3.28, 0.00, ±3.12. The density distribution conforms to the assumed C_{2v} molecular symmetry with the twofold axis along the x direction and the normals of the mirror planes along the y and z directions. Based on the assumption that the ground state $|\Psi_0\rangle$ contains one electron, the scale (in units of $e^-/(au)^3$) for the contour lines on each map decreases by a factor of 2 for each successive line from a maximum value of 0.500 for A to 0.610×10^{-4} for N.

Although the computed values for the mixing coefficients have been shown to be dependent upon the axial labeling scheme, the directional properties of $|\Psi_0\rangle$ and its electron density are rotationally invariant to the choice of the coordinate system. Contour maps of either $|\Psi_0\rangle$ or its electron density are identical for the three possible permutations of x, y, and z. In order to visualize the spatial distribution of the unpaired electron on the metal for $V(\eta^5\text{-}C_5H_4CH_3)_2Cl_2$, the electron-density contour maps, shown in Figure 9 for the xz, xy, and yz planes, were calculated[37] for $|\Psi_0\rangle = -0.976d_{z^2} + 0.218d_{x^2-y^2}$.

Table X. Summary of Single-Crystal and Glass EPR Data for $M(\eta^5\text{-}C_5H_5)_2L_2$ (M = V, Nb) with "Best-Fit" Parameters

Ref	Molecule	T_x[a,b]	T_y	T_z	$a(d_{z^2})$	$b(d_{x^2-y^2})$	a^2/b^2	λ (cm^{-1})	P[d]	K[d]	$\langle r^{-3}\rangle$[e]	χ
This work	$V(\eta^5\text{-}C_5H_4CH_3)_2Cl_2$	−80.6	−125.5	−20.5	−0.976	0.218	20.0	61	97.0	68.8	2.07	−2.21
		(−80.8)	(−125.4)	(−20.6)[c]								
5	$V(\eta^5\text{-}C_5H_5)_2S_5$	−66.6	−111.3	−23.5	−0.963	0.270	12.7	30	87.1	61.5	1.86	−1.97
		(−66.6)	(−111.3)	(−23.5)								
41	$V(\eta^5\text{-}C_5H_5)_2Cl_2$	−80.1	−127.2	−28.6	−0.967	0.255	14.4	110	93.8	69.5	2.00	−2.23[f]
		(−80.0)	(−127.2)	(−28.6)								
40	$V(\eta^5\text{-}C_5H_5)_2Cl_2$	−79.2	−125.2	−16.3	−0.977	0.213	21.0	50	101.0	67.1	2.16	−2.15
		(−79.3)	(−125.1)	(−16.2)								
40	$V(\eta^5\text{-}C_5H_5)_2(SCN)_2$	−76.2	−123.3	−20.5	−0.973	0.231	17.7	60–70	93.8	66.7	2.01	−2.14
		(−76.0)	(−123.4)	(−20.6)								
40	$V(\eta^5\text{-}C_5H_5)_2(OCN)_2$	−78.5	−127.7	−19.9	−0.973	0.231	17.7	60–70	98.4	68.3	2.10	−2.19
		(−78.4)	(−127.8)	(−20.0)								
40	$V(\eta^5\text{-}C_5H_5)_2(CN)_2$	−62.8	−106.0	−11.8	−0.971	0.239	16.5	<40	88.1	55.5	1.88	−1.78
		(−62.4)	(−106.2)	(−12.0)								
40	$Nb(\eta^5\text{-}C_5H_5)_2Cl_2$	−114.0	−170.9	−56.5	−0.968	0.251	14.9	110–150	102.8	103.4	2.36	−3.57
		(−114.0)	(−171.0)	(−56.5)								
40	$Nb(\eta^5\text{-}C_5H_5)_2(SCN)_2$	−107.5	−164.3	−56.5	−0.965	0.262	13.6	110–160	96.2	99.6	2.21	−3.43
		(−107.6)	(−164.3)	(−56.5)								
40	$Nb(\eta^5\text{-}C_5H_5)_2(\sigma\text{-}C_5H_5)_2$	−97.1	−153.1	−46.8	−0.960	0.280	11.8	<110	99.3	91.0	2.28	−3.14
		(−96.9)	(−153.2)	(−46.9)								
40	$Nb(\eta^5\text{-}C_5H_5)_2(CN)_2$	−82.5	−138.3	−57.1	−0.932	0.363	6.6	<110	77.3	85.7	1.78	−2.96
		(−81.9)	(−138.8)	(−57.2)								

[a] Hyperfine components are given in units of gauss. [b] Data from ref 40 and 41 were converted from units of 10^{-4} cm^{-1} to gauss through division by the factor 0.9348 (g/g_e) where g_e = 2.0023. [c] Numbers in parentheses are the calculated components obtained for the "best" values of a and b. [d] Given in units of 10^{-4} cm^{-1}. [e] Given in atomic units (au). [f] The χ value of −2.08 reported in ref 41 was calculated from the isotropic coupling determined by J. C. W. Chien and C. R. Boss, *J. Am. Chem. Soc.*, 83, 3767 (1961), from the solution EPR spectrum of $V(\eta^5\text{-}C_5H_5)_2Cl_2$ rather than from the single-crystal EPR data.

Figure 9a graphically illustrates that the unpaired spin density on the metal is primarily directed along the z direction normal to the xy plane (which bisects the Cl-V-Cl bond angle) where the coordinates of the two chlorine atoms in atomic units are 3.28, 0.00, ±3.12. The significantly smaller spin density along the y direction substantiates the assumption that the methylcyclopentadienyl ring contribution to the MO containing the unpaired electron is sufficiently small to be neglected. However, since most of the spin density on the metal is localized in the xz plane, a significant interaction with the Cl ligands is possible, from which one can rationalize both the decrease in the L-M-L bond angle and the antibonding effect on the M-L bond distance as the number of electrons occupying this MO is increased.

The calculated value of $(-)K$ of −73.6 G for $V(\eta^5\text{-}C_5H_4CH_3)_2Cl_2$ agrees well with that of −72.8 G calculated from the solution EPR spectrum. The larger magnitude of K for $V(\eta^5\text{-}C_5H_4CH_3)_2Cl_2$ compared to that for $V(\eta^5\text{-}C_5H_5)_2S_5$ indicates that the unpaired electron is localized to a greater degree on the vanadium atom in $V(\eta^5\text{-}C_5H_4CH_3)_2Cl_2$. The P value for $V(\eta^5\text{-}C_5H_4CH_3)_2Cl_2$ of 103.8 G indicates that the effective nuclear charge on the vanadium atom is nearly +1.[38] In general, the expectation value of $1/r^3$, which is computed from P, decreases as the covalency of a series of related paramagnetic compounds increases. Hence, the decrease in $\langle r^{-3}\rangle$ from 2.07 au for $V(\eta^5\text{-}C_5H_4CH_3)_2Cl_2$ to 1.86 au for $V(\eta^5\text{-}C_5H_5)_2S_5$ indicates a greater covalency for the pentasulfide molecule. A negative value of χ has already been shown to be reasonable for V(IV) compounds.[38] However, since an admixture of 4s orbital character due to spin polarization effects introduces a positive contribution to χ,[39] the more negative χ value of −2.21 determined for $V(\eta^5\text{-}C_5H_4CH_3)_2Cl_2$ reflects a smaller contribution of 4s metal character into its ground state in comparison to that for $V(\eta^5\text{-}C_5H_5)_2S_5$, for which the determined χ value is −1.97.

The coincidence of **g** and **T** for $V(\eta^5\text{-}C_5H_4CH_3)_2Cl_2$ has made it possible to estimate an upper limit of the vanadium spin-orbit coupling constant. Because of the small variations of the principal components of **g** for both $V(\eta^5\text{-}C_5H_5)_2S_5$ and $V(\eta^5\text{-}C_5H_4CH_3)_2Cl_2$ from the free-electron value of 2.0023, the spin-orbit contributions from the vanadium nucleus are not expected to be appreciable in either molecule. The λ for $V(\eta^5\text{-}C_5H_5)_2S_5$ was previously estimated[5] to be ca. 30 cm^{-1}, but since the unpaired electron resides more on the vanadium atom in $V(\eta^5\text{-}C_5H_4CH_3)_2Cl_2$ than in $V(\eta^5\text{-}C_5H_5)_2S_5$ the spin-orbit coupling constant for the former molecule is most likely greater than 30 cm^{-1}. Since the spin density of the unpaired electron resides primarily on the vanadium atom, spin-orbit coupling terms for the Cl ligands were not included. In order to obtain a reasonable value for λ from the EPR data, the electronic transition energies, ΔE_{ij}'s, must be known. Although the electronic spectrum of $V(\eta^5\text{-}C_5H_4CH_3)_2Cl_2$ has not been studied, the visible-uv absorption spectra of several $V(\eta^5\text{-}C_5H_5)_2L_2$ complexes (L = Cl, SCN, OCN, CN) in dichloromethane solution have been reported[40] along with the observation that these spectra are very much alike; the ν_{max} values and their assigned transitions[40] (given in parentheses) for $V(\eta^5\text{-}C_5H_5)_2Cl_2$ are as follows: 11,800 (d-d transition), 13,600 (d-d transition), 26,300 (charge transfer from ring to V(IV)), and 35,400 cm^{-1}. From the "best" values of a and b (and the determined g_x, g_y, and g_z values) for $V(\eta^5\text{-}C_5H_4CH_3)_2Cl_2$, a value of 61 cm^{-1} for λ leads to calculated electronic energies of ΔE_{xz} = 11,973, ΔE_{yz} = 13,544, and ΔE_{xy} = 23,142 cm^{-1}, which are in reasonable agreement with the observed d-d transition energies for $V(\eta^5\text{-}C_5H_5)_2Cl_2$.

While these dilute single-crystal EPR studies of $V(\eta^5\text{-}C_5H_4CH_3)_2Cl_2$ were in progress, two papers appeared in the literature reporting the results and interpretation of EPR data for $M(\eta^5\text{-}C_5H_5)_2L_2$ species (M = V, Nb).[40,41] From their single-crystal EPR study of $V(\eta^5\text{-}C_5H_5)_2Cl_2$ doped in the crystal lattice of $Ti(\eta^5\text{-}C_5H_5)_2Cl_2$, Bakalik and Hayes[41] concluded that the unpaired electron is in an a_1-type MO primarily composed of $3d_{z^2}$ and $3d_{x^2-y^2}$ character. However, since the crystal structure of the diamagnetic

host $Ti(\eta^5\text{-}C_5H_5)_2Cl_2$ was not known at that time, they could not unambiguously assign the orientation of the magnetic tensors with respect to the $V(\eta^5\text{-}C_5H_5)_2Cl_2$ molecule in the crystal lattice and hence were not able to select a unique set of coefficients specifying the metal orbital character. An article by Stewart and Porte[40] discussed the dilute glass EPR spectra for several vanadium and niobium $M(\eta^5\text{-}C_5H_5)_2L_2$ molecules (L = Cl, SCN, OCN, $\eta^1\text{-}C_5H_5$, and CN). Due to the nature of this experiment when performed for paramagnetic species with less than axial symmetry, their assignment of the orientation of the principal axes for the magnetic sites appears to be an arbitrary one. The results of our EPR studies have shown, unfortunately, that their assumption that the z component of **g** and **T** coincides with the C_2-2 axes of the molecules is incorrect. However, the magnitudes of the hyperfine components which they determined for $V(\eta^5\text{-}C_5H_5)_2Cl_2$ from a computer simulation of its dilute glass spectrum are comparable to those obtained from our dilute single-crystal EPR study of $V(\eta^5\text{-}C_5H_4CH_3)_2Cl_2$.

Table X summarizes all of the dilute single-crystal and glass EPR data that have been obtained for the hyperfine coupling tensor for d^1 M(IV) $M(\eta^5\text{-}C_5H_5)_2L_2$ complexes (M = V, Nb). From the same expressions given elsewhere,[42] the "best" values for the mixing coefficients, a and b, as well as the values for P, K, $\langle r^{-3}\rangle$, and χ have been computed for each of these complexes. Although the magnitude of the mixing coefficients vary somewhat depending upon the ligand L, the similar anisotropy in the **T** tensor indicates that the metal orbital character of the unpaired electron is not appreciably affected. The calculated values in Table X for P, K, $\langle r^{-3}\rangle$, and χ are all reasonable. The lower values of P, K, $\langle r^{-3}\rangle$, and χ for the vanadium and niobium cyanide complexes are consistent with a greater delocalization of the unpaired electron on the CN ligands for these molecules.

Acknowledgments. We gratefully acknowledge the financial support of this research by the National Science Foundation (No. GP-19175X). We also wish to express our appreciation to Professors Malcolm H. Green (Oxford), John E. Harriman (University of Wisconsin, Madison), John A. Weil (University of Saskatchewan), and Mr. James Kleppinger (University of Wisconsin, Madison) for helpful discussions. J.L.P. wishes to thank the National Science Foundation for a predoctoral National Science Foundation Traineeship.

Supplementary Material Available. A listing of the observed and calculated structure factor amplitudes will appear following these pages in the microfilm edition of this volume of the journal. Photocopies of the supplementary material from this paper only or microfiche (105 × 148 mm, 24× reduction, negatives) containing all of the supplementary material for the papers in this issue may be obtained from the Business Office, Books and Journals Division, American Chemical Society, 1155 16th St., N.W., Washington, D.C. 20036. Remit check or money order for $4.00 for photocopy or $2.50 for microfiche, referring to code number JACS-75-6422.

References and Notes

(1) (a) Presented in part at the 6th International Conference on Organometallic Chemistry, University of Massachusetts, Aug 1973; (b) based in part on a dissertation submitted by J. L. Petersen to the Graduate School of the University of Wisconsin in partial fulfillment of the requirement for the Ph.D. degree, May 1974.
(2) (a) E. G. Muller, Ph.D. Thesis, University of Wisconsin (Madison), 1970; (b) E. G. Muller, S. F. Watkins, and L. F. Dahl, *J. Organometal. Chem.*, in press; (c) E. G. Muller, J. L. Petersen, and L. F. Dahl, *J. Organometal. Chem.*, in press.
(3) C. J. Ballhausen and J. P. Dahl, *Acta Chem. Scand.*, **15**, 1333 (1961).
(4) L. F. Dahl, Plenary Lecture, 4th International Conference on Organometallic Chemistry, Bristol, 1969.
(5) J. L. Petersen and L. F. Dahl, *J. Am. Chem. Soc.*, **97**, 6416 (1975).
(6) G. Doyle and R. S. Tobias, *Inorg. Chem.*, **7**, 2479 (1968).
(7) Our synthesis and subsequent characterization of the methylcyclopentadienyl titanium and vanadium dichloride complexes originated from our photoelectron spectroscopy studies, which were being performed in conjunction with nonparameterized Fenske–Hall MO calculations, on $M(\eta^5\text{-}C_5H_5)_2Cl_2$ (M = Ti, V). In order to obtain sufficient sample pressures in the spectrometer the compounds were heated to 150°. However, while $Ti(\eta^5\text{-}C_5H_5)_2Cl_2$ readily sublimes at this temperature, $V(\eta^5\text{-}C_5H_5)_2Cl_2$ undergoes thermal decomposition to a blue-green substance, possibly $V(\eta^5\text{-}C_5H_5)_2$ or $V(\eta^5\text{-}C_5H_5)_2Cl$, with an entirely different solution EPR spectrum than that for $V(\eta^5\text{-}C_5H_5)_2Cl_2$. From conversations with Dr. Malcolm Green (a visiting Professor at Harvard from Oxford University during the spring semester, 1973), we learned that similar PES studies of $M(\eta^5\text{-}C_5H_5)_2Cl_2$ (M = Nb, Mo) by Dr. J. C. Green (Oxford) also were initially hindered by thermal decomposition of the niobium complex but that this decomposition problem was remedied by the preparation of the more volatile methylcyclopentadienyl analogs. In addition, we hoped that the replacement of the unsubstituted cyclopentadienyl rings by methylcyclopentadienyl ones in these dichloride complexes would eliminate the twinning problem which had been previously encountered[8] in the solid state for $Ti(\eta^5\text{-}C_5H_5)_2Cl_2$.
(8) A. Clearfield, D. K. Warner, C. H. Saldarriaga-Molina, R. Gopal, and I. Bernal, submitted for publication.
(9) J. J. Eisch and R. B. King, "Organometallic Synthesis", Vol. 1, Academic Press, New York, N.Y., 1965, p 75.
(10) The magnetic susceptibility measurements were carried out by Mr. J. Kleppinger, Department of Chemistry, University of Wisconsin (Madison).
(11) M. J. Camp, Ph.D. Thesis, University of Wisconsin (Madison), 1972.
(12) A. Earnshaw, "Introduction of Magnetochemistry", Academic Press, New York, N.Y., 1968, pp 5–6; P. W. Selwood, "Magnetochemistry", 2nd ed, Interscience, New York, N.Y., 1956, p 78.
(13) J. A. Weil, *J. Magn. Reson.*, **4**, 394 (1971).
(14) J. C. Calabrese, "FOBS, General Data Reduction Program for Raytheon 706", University of Wisconsin (Madison), 1972.
(15) J. C. Calabrese, "SORTMERGE", Ph.D. Thesis (Appendix), University of Wisconsin (Madison), 1971.
(16) J. F. Blount, "DEAR", based on a method given by W. R. Busing and H. A. Levy, *Acta Crystallogr.*, **10**, 180 (1957).
(17) "PREDEAR, Preliminary Absorption Program", adapted from Blount's "DEAR" program.
(18) J. C. Calabrese, "PHASE, Patterson Heavy Atom Solution Extractor", Ph.D. Thesis (Appendix), University of Wisconsin (Madison), 1971.
(19) J. C. Calabrese, "MAP, An Integrated Structure Factor, Fourier, Peaksearch, and Fourier Connectivity Program", University of Wisconsin (Madison), 1972.
(20) (a) J. C. Calabrese, "A Crystallographic Variable Matrix Least-Squares Refinement Program", University of Wisconsin (Madison), 1972; (b) W. R. Busing, K. O. Martin, and H. A. Levy, "ORFLS, A Fortran Crystallographic Least-Squares Program," ORNL-TM-305, Oak Ridge National Laboratory, Oak Ridge, Tenn., 1962.
(21) $R_1 = [\Sigma||F_o| - |F_c||/\Sigma|F_o|] \times 100$ and $R_2 = [\Sigma w_i||F_o| - |F_c||^2/\Sigma w_i|F_o|^2]^{1/2} \times 100$. All least-squares refinements were based on the minimization of $\Sigma w_i||F_o| - |F_c||^2$ with the individual weights $w_i = 1/\sigma(|F_o|)^2$.
(22) J. C. Calabrese, "MIRAGE", Ph.D. Thesis (Appendix), University of Wisconsin (Madison), 1971.
(23) The scattering factor tables used for all nonhydrogen atoms were those of Cromer et al.[24] while those for the hydrogen atoms were from Stewart et al.[25] Real and imaginary corrections for anomalous dispersion (viz., $\Delta f' = 0.3$, $\Delta f'' = 0.6$ for Ti; $\Delta f' = 0.3$, $\Delta f'' = 0.7$ for V; and $\Delta f' = 0.1$, $\Delta f'' = 0.2$ for Cl)[26] were included in the structure factor calculations.
(24) D. T. Cromer and J. B. Mann, *Acta Crystallogr., Sect. A*, **24**, 321 (1968).
(25) R. F. Stewart, E. R. Davidson, and W. T. Simpson, *J. Chem. Phys.*, **42**, 3175 (1965).
(26) "International Tables for X-Ray Crystallography", Vol. III, Kynoch Press, Birmingham, 1968, p 215.
(27) For a listing of the observed and calculated structure factors, see paragraph at end of paper regarding supplementary material.
(28) W. R. Busing, K. O. Martin, and H. A. Levy, "ORFFE, A Fortran Crystallographic Function and Error Program", ORNL-TM-306, Oak Ridge National Laboratory, Oak Ridge, Tenn., 1964.
(29) D. L. Smith, "PLANES", Ph.D. Thesis (Appendix IV), University of Wisconsin (Madison), 1962.
(30) C. K. Johnson, "ORTEP, A Fortran Thermal Ellipsoid Plot Program for Crystal Structure Illustration", ORNL-3794, Oak Ridge National Laboratory, Oak Ridge, Tenn., 1964.
(31) For the two crystallographic independent $Ti(\eta^5\text{-}C_5H_5)_2Cl_2$ molecules the average Ti–Cl and Ti–Cp(c) distances are 2.364 and 2.059 Å, respectively, while the average Cl–Ti–Cl, Cp(c)–Ti–Cp′(c), and Cp(c)–Ti–Cl angles are 94.5, 131.0, and 106.4°, respectively.
(32) B. R. Davis and I. Bernal, *J. Organomet. Chem.*, **30**, 75 (1971).
(33) E. F. Epstein, I. Bernal, and H. Köpf, *J. Organomet. Chem.*, **26**, 229 (1971).
(34) L. Pauling, "The Nature of the Chemical Bond", 3rd ed, Cornell University Press, Ithaca, N.Y., 1960.
(35) H. Goldstein, "Classical Mechanics", Wiley, New York, N.Y., 1965, p 107.
(36) (a) P. C. Taylor and P. J. Bray, Lineshape Program Manual, Physics Department, Brown University, 1968 (unpublished); (b) P. C. Taylor and P. J. Bray, *J. Magn. Reson.*, **2**, 305 (1970); (c) P. C. Taylor, private communication to J. L. P., 1973; P. C. Taylor, J. F. Baugher, and H. F. Kriz, *Chem. Rev.*, **75**, 203 (1975).
(37) Contour maps were calculated and plotted with the aid of "MOPLOT", D. L. Lichtenberger, Ph.D. Thesis (Appendix), University of Wisconsin

(Madison), 1974.
(38) (a) B. R. McGarvey, *J. Phys. Chem.*, 71, 51 (1967); (b) A. Abragam and B. Bleaney, "Electron Paramagnetic Resonance of Transition Ions", Claredon Press, Oxford, 1970, p 706.
(39) A. Abragam and B. Bleaney, ref 38b, p. 399.
(40) C. P. Stewart and A. L. Porte, *J. Chem. Soc., Dalton Trans.*, 722 (1973).
(41) D. P. Bakalik and R. G. Hayes, *Inorg. Chem.*, 11, 1734 (1972).
(42) See Table II in ref 5.

Nonparameterized Molecular Orbital Calculations and Photoelectron Spectroscopy of Open- and Closed-Shell M(IV) $M(\eta^5\text{-}C_5H_5)_2L_2$ Complexes[1]

Jeffrey L. Petersen, Dennis L. Lichtenberger, Richard F. Fenske, and Lawrence F. Dahl*

Contribution from the Department of Chemistry, University of Wisconsin, Madison, Wisconsin 53706. *Received February 24, 1975*

Abstract: Nonparameterized (Fenske-Hall)-type molecular orbital calculations have been performed on several d^0, d^1, and d^2 M(IV) $M(\eta^5\text{-}C_5H_5)_2L_2$ molecules, and the results have been found to be completely compatible with the interpretations obtained from the electron paramagnetic resonance and photoelectron spectral measurements as well as from the crystallographically acquired bond-length and bond-angle data. The MO calculations reveal that the LUMO for the d^0 Ti(IV) complexes and the HOMO for the d^1 and nonhydridic d^2 M(IV) complexes possess analogous orbital characters principally associated with the metal d_{z^2} and $d_{x^2-y^2}$ AO's with considerable contributions from the 3p AO's of the sulfur or chlorine L ligands. The *relative* metal orbital compositions of the HOMO's in the open-shell d^1 V(IV) complexes are in remarkable agreement with those obtained from our previously reported dilute single-crystal EPR studies on $V(\eta^5\text{-}C_5H_5)_2S_5$ and $V(\eta^5\text{-}C_5H_4CH_3)_2Cl_2$. For $V(\eta^5\text{-}C_5H_5)_2S_5$ the per cent character ratio of $3d_{z^2}/3d_{x^2-y^2}$ = 12.7/1 (EPR) vs. 7.7/1 (MO), while the corresponding ratio of 20.0/1 from the EPR data on $V(\eta^5\text{-}C_5H_4CH_3)_2Cl_2$ compares with that of 20.5/1 from the MO computations. Additional information concerning the electronic structure of $M(\eta^5\text{-}C_5H_5)_2L_2$ complexes has been obtained from photoelectron spectroscopy. The PE spectra of $M(\eta^5\text{-}C_5H_5)_2Cl_2$ and $M(\eta^5\text{-}C_5H_4CH_3)_2Cl_2$ (where M = Ti, V) are presented and interpreted with the aid of the approximate MO calculations.

Dilute single-crystal EPR studies of $V(\eta^5\text{-}C_5H_5)_2S_5$[2] and $V(\eta^5\text{-}C_5H_4CH_3)_2Cl_2$[3] have provided a *quantitative* determination of the relative metal orbital character for the unpaired electron in these d^1 V(IV) molecules. Although the d^1 electron occupies a molecular orbital of predominately metal character,[2,3] there is appreciable evidence which indicates that the composition of the highest occupied molecular orbital (HOMO) is not restricted solely to the $3d_{z^2}$ and $3d_{x^2-y^2}$ metal AO's but contains a significant orbital contribution from the L ligands. The presumed antibonding effect of the unpaired electron on the V-L bond length (rationalized from a bond-length comparison between the corresponding d^0 Ti(IV) and d^1 V(IV) pentasulfide and chloride complexes), the variation of 60–75 G in the ^{51}V isotropic hyperfine coupling constant for different $V(\eta^5\text{-}C_5H_5)_2L_2$ complexes, and the noticeably larger line widths for the hyperfine lines of $V(\eta^5\text{-}C_5H_4CH_3)_2Cl_2$ in comparison to those of $V(\eta^5\text{-}C_5H_5)_2S_5$ are all reasonable indications of partial delocalization of the unpaired electron onto the L ligands.

The fact that approximate molecular orbital calculations coupled with photoelectron spectroscopy were successfully utilized[4] in a characterization of the electronic structure and bonding in a number of transition metal carbonyl complexes prompted us to apply these methods to representative $M(\eta^5\text{-}C_5H_5)_2L_2$ complexes. The Fenske-Hall MO procedure[5] does not involve the use of empirical or variable parameters; the final results, which are invariant to a rotation of the local coordinate system on each atom, depend only upon the choice of basis functions and the interatomic distances.[6,7] This MO method applied to $M(\eta^5\text{-}C_5H_5)_2S_5$, $M(\eta^5\text{-}C_5H_5)_2(SC_6H_5)_2$, $M'(\eta^5\text{-}C_5H_5)_2Cl_2$ (M = Ti, V; M' = Ti, V, Cr, Mo), and $Mo(\eta^5\text{-}C_5H_5)_2H_2$ has made possible a comparison of the calculated per cent metal orbital characters for the HOMO in the d^1 V(IV) molecules with those experimentally determined from the dilute single-crystal EPR studies. Our main goals were: (1) to estimate the degree of delocalization of the unpaired electron on the ligands (which cannot be directly determined in the absence of ligand hyperfine interaction from the EPR data) from the calculated orbital character of the ligand atoms in the HOMO; and (2) to determine to what extent the composition of the HOMO is affected as the population in the HOMO is varied from 0 to 2 electrons.

Additional experimental information about the electronic structure of $M(\eta^5\text{-}C_5H_5)_2L_2$ complexes has been obtained by means of photoelectron spectroscopy. The PE spectra of $M(\eta^5\text{-}C_5H_5)_2Cl_2$ and $M(\eta^5\text{-}C_5H_4CH_3)_2Cl_2$ (M = Ti, V) are presented and interpreted with the aid of the results from the (Fenske-Hall)-type molecular orbital calculations.

Experimental Section

Photoelectron Spectral Characterization. The photoelectron spectra were measured with a Varian IEE-15 electron spectrometer in the uv configuration. The helium source was pure to 0.0001%. Simultaneous observation of a number of reference gas ionization peaks indicated the energy scale to be linear within less than 0.01 eV over a range of binding energies from 9 to 17 eV. Argon was used as a single *internal* standard (15.76 eV peak) in order to check the spectrometer's resolution as well as its sensitivity. Because of the nature of the compounds used, the samples had to be heated to at least 150° in order to attain sufficient sample vapor pressure in the spectrometer. The samples were heated slowly until reasonable counting rates were reached. Before a sample was introduced into the spectrometer, however, the thermal stability of the compound was checked by vacuum sublimation of the compound at 150°. PE spectra for $Ti(\eta^5\text{-}C_5H_5)_2S_5$ and $Ti(\eta^5\text{-}C_5H_5)_2(SC_6H_5)_2$ were not obtained because of thermal decompo-